Centre for Geo-Information

Thesis Report GIRS-2005-2

EVALUATING THE APPLICABILITY OF MODIS DATA FOR PHENOLOGICAL MONITORING IN THE NETHERLANDS

Angela Susanna Eugenie Kross

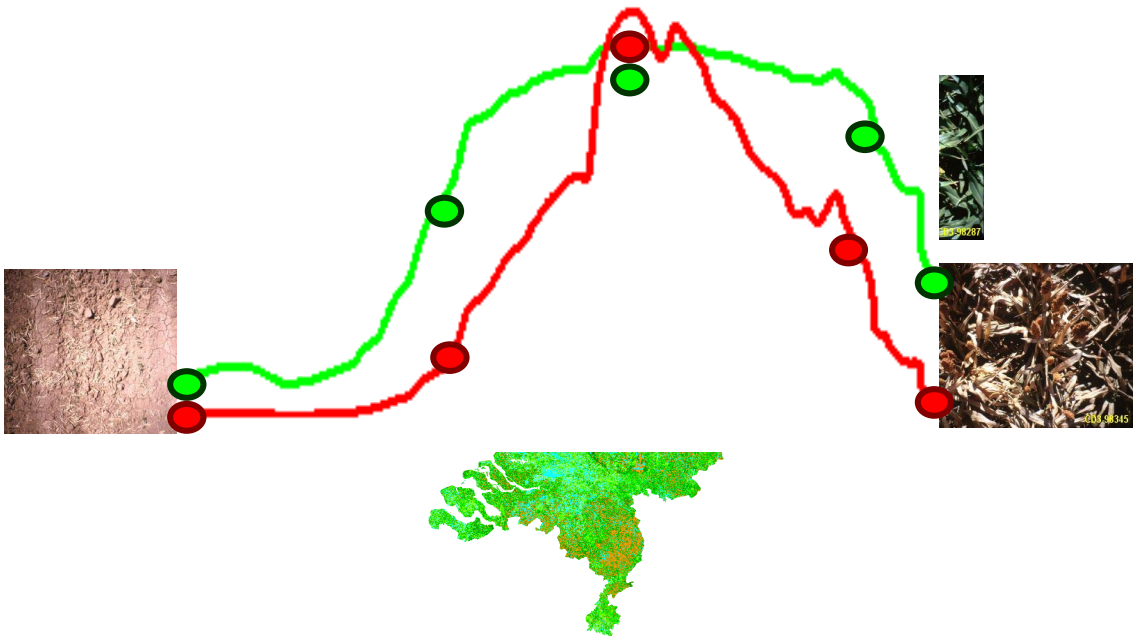

March 2005

WAGENINGEN UNIVERSITY
WAGENINGEN UR

EVALUATING THE APPLICABILITY OF MODIS DATA FOR PHENOLOGICAL MONITORING IN THE NETHERLANDS

Angela Susanna Eugenie Kross

Registration number 72 04 29 482 110

Supervisors:

Drs. A. J. W. de Wit

Dr. Ir. J. G. P. W. Clevers

A thesis submitted in partial fulfillment of the degree of Master of Science at Wageningen University and Research Centre, The Netherlands.

March 2005

Wageningen, The Netherlands

Thesis code number: GRS-80337
Wageningen University and Research Centre
Laboratory of Geo-Information Science and Remote Sensing
Thesis Report: GIRS-2005-2

"Só podemos ter certeza da nossa capacidade quando nos colocamos in acão. Pois é através do trabalho que descrobimos os talentos e as habilidades que animam o nosso espírito"

Paulo Vitor

ACKNOWLEDGEMENT

Many people contributed in different ways to the development of this study and I hereby would like to acknowledge all for their direct or indirect participation. Special emphasis I would like to give to the following people and institutions.

First of all I would like to acknowledge the Nuffic-NFP program. Thanks to this funding I was enabled to participate in this study program. My sincere gratitude goes to my supervisors for guiding me towards my objectives: Allard de Wit, for his dedication in supporting and discussing my aspirations and Jan Clevers for keeping me on the track in a consistent and constructive way. I owe many thanks to Arnold van Vliet and Mark Grutters for providing the field data. Without this information the study would have been incomplete. Also my special thanks to Jin Chen for his readiness to provide me with his smoothing method. During the progress of my work I have received many useful suggestions, comments and information, and my special thanks goes to: Willy ten Haaf, Bram van Putten, Gerard Heuvelink, Arnold Bregt, Gerrit Gort, Frans Rip and Bradley Reed. During the long days at Alterra, studying became a pleasure and my motivation was significantly improved by the presence of my dear colleagues: Taye, Lucinka, Jie, Teshome, Babs, Tine, Elisa, Worku & Jochem. My deepest gratitude goes to my family. To Silvia and Frederik, for their readiness in supporting me with everything. Words can not explain the extent. To Robert, for his readiness to criticize and question all and everything in an inconsistent and sometimes constructive way. To Ineke, Pearl, Julio and Santino. My special consideration and thanks goes to Mamadou for his overall patience (most of the times), understanding and support. And finally, I dedicate this work to my late parents: the fruits of the education I have received are everlasting...

ABSTRACT

The phenological timing of vegetation has an important role within global ecosystem models and vegetation monitoring. Within this scope, remote sensing (RS) techniques have shown their potential for the monitoring of broad scale vegetation conditions. However, the understanding of the relation between remote sensing phenology and surface phenology remains unclear and limits the full usefulness of the potential of remotely sensed data. Within this context, the present study was conducted with the objective to evaluate the applicability of the MODerate resolution Imaging Spectroradiometer sensor (MODIS) data for phenological monitoring in the Netherlands. To achieve the objectives the study was accomplished on deciduous forest, grassland and winter wheat in the Netherlands from 2000 to 2004. MODIS 16-day Normalized Difference Vegetation Index (NDVI) and Enhanced Vegetation Index (EVI) composites with a spatial resolution of 250 m. were smoothed by two methods: the Harmonic ANalysis of Time Series algorithm (HANTS) and the Savitszky Golay filter based method (SG). From the smoothed data we derived the Start Of the growing Season (SOS), End Of the growing Season (EOS) and Growing Season Length (GSL) by two estimation methods: the Seasonal Midpoint NDVI (SMN) and the Maximum increase (MI). Finally, the summary statistics were calculated and trend analyses were realized on “pure” vegetation classes. The reliability of the remote sensing phenological indicators (RSPIs) was defined in relation to field and model data. The results showed the potential of the RS data in capturing the general interannual surface phenology. The relatively late leaf unfolding (UL) and flowering (F) periods in 2001 were identified at all studied classes. The early UL and F periods in 2002 were also depicted at al classes. The smaller variations were not captured by any of the methods, most likely due to the temporal resolution of the MODIS data. With regard to the different vegetation classes, the following conclusions could be drawn: (1) For the deciduous forest, the EVI in combination with the HANTS (EVI_HANTS) and any of the estimation methods performed best. Mean UL and F trends were simulated within the SOS interval. (2) The grassland cover was more difficult to be related to the RS phenology, but the EVI_HANTS methods also showed good performance and simulated the mean flowering trend within one 16-day unit earlier. (3) For the winter wheat, the RS phenology did not succeed in a consistant simulation of the model SOS. The model EOS was best simulated by the combination of the EVI with the SG. With regard to the method combinations we conclude that: (1) In general, The EVI based RSPIs appeared to be more sensitive for variances in the vegetation status and seem to overcome the time unit constraint for detection of the general interannual phenology trend. (2) For monitoring of the mean UL and F dates the combination of the EVI with the HANTS and the MI method showed superior performance for all vegetation classes. (3) The SG based methods performed well in reconstructing the Vegetation index (VI) time series. However, the estimation methods were not found suitable for the derivation of the RSPIs based on the SG smoothed data. This method has its potential in providing more accurate information on phenological metrics as: maximum NDVI and multi modality. The results were found promising, but it is expected that further studies, mainly on the relationships between the surface phenophases and the vegetation indices / RSPIs and based on images with a higher temporal resolution should increase the understanding of the relationship between remote sensing phenology and surface phenology.

KEYWORDS: Phenology, Remote sensing, MODIS, NDVI, EVI, HANTS, Savitzky Golay filter

INDEX

LIST OF FIGURES

LIST OF TABLES

LIST OF EQUATIONS

LIST OF ABBREVIATIONS

ARVI	Atmospherically Resistant Vegetation Index
AVHRR	Advanced Very High-Resolution Radiometer
BF	Beginning of Flowering / of blossom; first flowers open
BISE	Best Index Slope Extraction
CL	Colouring of Leaves
CL50	Colouring of Leaves - 50 % of total
CL100	Colouring of Leaves – 100 % of total
CV	Coefficient of Variance
CV-MVC	Constraint-View angle Maximum Value Compositing
d	Parameter for the Savitzky-Golay smoother: degree of the smoothing polynomial
DMA	Delayed Moving Average
DOY	Day Of Year (Julian days)
EF	End of Flowering / of blossom
ENVI	The Environment for Visualizing Images
IDL	Interactive Data Language
EOS - HDF	Earth Observing system – Hierarchical Data Format
ERDAS	Earth Resources Data Analysis System
EVI	Enhanced Vegetation Index
FET	Fit Error Tolerance: is maximum tolerable downward deviation between fourier fit and NDVI data values (in DN values)
FF	Full Flowering / General flowering / Full blossom
FFM	Fourier Fitting Method
FFT	Fast Fourier Transform
FL	Leaf Fall
fPAR	fraction of Photosynthetic Active Radiation absorbed by the green vegetation canopy
FREQS	1D array with frequencies that should be selected from the fourier spectrum. i.e. fregs = [0,1,2] to use the fourier components 0 (mean), 1 (1 sine wave), 2 (2 sine waves).
GEMI	Global Environmental Monitoring Index
GSL	Growing Season Length
HANTS	Harmonic ANalysis of Time Series algorithm
HDF	Hierarchical Data Format
IMAX	Maximum nr. Of Iteration to be performed during processing
KNMI	Koninklijke Nederlandse Meteorologisch Instituut
LAI	Leaf Area Index
m	Parameter for the Savitzky-Golay smoother: half width of the smoothing window
MERIS	Medium Resolution Imaging Spectrometer
MI	Maximum Increase: estimation method for the Start of the Growing Season
MODIS	The MODerate resolution Imaging Spectroradiometer sensor
MRT	Modis Reprojection Tool
MSR	Modified Simple Ratio
NDVI	Normalized Difference Vegetation Index
NLI	Non Linear vegetation Index
NOAA	National Oceanic and Atmospheric Administration's
QA	Quality Assessment images

RANGE	Array of size 2 to specify to specify the minimum and maximum valid data values. i.e. range=[1,254]
RDVI	Renormalized Difference Vegetation Index
RP	Fruit Ripe for picking (pome fruit, sweet cherry, morello, red currant)
RP	First Ripe Fruits (European chestnut, almond)
RSPIs	Remote Sensing based Phenological Indicators
SARVI	Soil and Atmospherically Resistant Vegetation Index
SAVI	Soil Adjusted Vegetation Index
SG	Savitzky – Golay filter based method
SL	Sprouting of Leaves
SMA	Spectral Mixture Analysis
SMN	Seasonal Midpoint NDVI – Normalized difference vegetation index
SMVI	Seasonal Midpoint Vegetation Index
SOS	Start of the growing season
SPOT	Satellite Pour l'Observation de la Terre – Earth Observation Satellite
SR	Simple Ratio
TAT	Throw Away Threshold, is maximum number of NDVI observations that can be discarded in the fitting process
TM	Landsat Thematic Mapper
UL	Beginning of the unfolding of the leaves, first leaf surfaces visible
VI	Vegetation Index
Vis	Vegetation Indices
WDVI	Weighted Difference Vegetation Index

1 INTRODUCTION

Phenology is the science of the timing of recurring biological phases (phenophases) and their causes. The importance of this science is widely recognized and it is extensively applied within related fields like agriculture, forestry, ecology and health (Van Vliet et al., 2003). Recently, this traditional science emerged as a new element within the research area of global modelling, monitoring and climate change. This is primarily due to its demonstrated high potential as an indicator of global climate change, but also due to the development of remote sensing technologies.

Remote sensing technologies can generate extensive biosphere-related databases; however, careful calibration and interpretation of this data is required to enable full profit of their research potential. Furthermore, remote sensing techniques should be seen as a complement to the traditional phenological observation methods: field measurements and phenological models (Schwartz, 1999). None of these methods individually can meet the needs of all research questions. Though, an integrative approach that combines the different observation methods can provide synergistic benefits (Schwartz, 2003). This approach requires sound understanding of the relationship between the different types of indicators (field phenological indicators, model phenological indicators and remote sensing phenological indicators).

It is within this scope that the present research will be conducted by studying remote sensing data acquired from the The MODerate resolution Imaging Spectroradiometer sensor (MODIS) and its applicability for the monitoring of vegetation phenology in the Netherlands.

1.1 PROBLEM CONTEXT AND DEFINITION

Phenological indicators can be derived by three main methods: field observations, phenology model outputs and remote sensing techniques.

❖ Phenological indicators derived from field measurements

Traditional phenological monitoring is realized by analyzing ground measurement data of the different phenological phases. The observation of phenophases in the field is labour-intensive and time consuming. In addition, comparability of the datasets is not always feasible due to different observation standards and gaps in observation data. However, it is the field data which are needed for calibration and validation of indicators coming from other methods. Therefore, even though the other methods are less time consuming, continuous efforts should be made on the improvement of the field measurement methods to minimize the current limitations. In the Netherlands, field phenological observations can be assessed through the Natuurkalender[1].

[1] www.natuurkalender.nl

Table 1-1 gives an overview of different standardized phases defined by the European Phenology Network (EPN, 2004).

Table 1-1. Overview of phenological phases of plants

SL	Sprouting of leaves
UL	Beginning of the unfolding of the leaves, first leaf surfaces visible
BF	First flowers open Beginning of flowering / of blossom
FF	Full flowering / General flowering / Full blossom
EF	End of flowering / of blossom
RP	Fruit ripe for picking (pome fruit, sweet cherry, morello, red currant)
RP	First ripe fruits (European chestnut, almond)
CL	Colouring of leaves
FL	Leaf fall

Source: Http://www.dow.wau.nl/msa/gpm, 21/06/2004

❖ Phenological indicators derived by phenology modelling

In 1735 Reaumur suggested that the differences between years and locations in the date of phenological events could be explained by differences in daily temperatures from an arbitrary date to the date of the phenological event considered. This suggestion is accepted till today as the main assumption in phenology modelling (Schwartz, 2003). Most plant phenology models predict budburst (leaf unfolding), flowering, and fruit maturation but were mainly developed for woody species rather than non-woody species (Schwartz, 2003). In general, many phenology models have been developed and applied with promising results. But according to Chuine (2000), the lack of standardization in phenology modelling implies difficulties in comparing and testing the model predictions.

❖ Phenological indicators derived by Remote sensing techniques

Differently from the traditional phenology monitoring methods, remote sensing techniques provide phenological data on a regional / global scale. The relation between surface phenology and remote sensing phenology is usually measured by Vegetation Indices (Table 1-2). Remote sensing studies on phenological monitoring started in the mid 1980s (Justice et al.., 1984; Mauser, 1986; Justice et al.., 1986; Townshend and Justice, 1986; Justice et al.., 1989) and were mainly based on images from the National Oceanic and Atmospheric Administration's (NOAA) advanced very high-resolution radiometer (AVHRR). Current researches are exploring the different improved and newly launched sensors and different estimation methods in order to come to more accurate methods for phenological monitoring (Ricotta and Avena, 2000; Privette et al., 2002; Huete et al., 2002; Zhang et al., 2003; Blanch Roure, 2003; Schwartz et al., 2003; De Wit and Su, 2004).

Table 1-2. Overview of remote sensing phenological indicators and their phenological interpretation, adapted from Reed (1994) and US. Department of the interior (2005).

Class	Remote sensing phenological indicator	Phenological interpretation
Temporal VI* indicators	Time of Start of Season (SOS) in Julian day	Beginning of measurable photosynthesis
	Time of End of Season (EOS) in Julian day	Cessation of measurable photosynthesis
	Duration of Growing Season (GSL) in days	Duration of photosynthetic activity
	Time of maximum VI (greenness) in Julian day	Time of maximum measurable photosynthesis
VI – value indicators	VI at start of growing season	Level of photosynthetic activity at SOS
	VI at end of growing season	Level of photosynthetic activity at EOS
	Maximum VI	Maximum measurable level of photosynthetic activity
	Range of VI	Range of measurable photosynthetic activity
Derived indicators	Time integrated NDVI	Net primary production
	Rate of greenup	Acceleration of photosynthesis
	Rate of senescence	Deceleration of photosynthesis
	Modality	Periodicity of photosynthetic activity

*VI = Vegetation index

The review on this subject evidenced numerous studies focussing on the applicability of the available sensors and estimation methods of phenological indicators. However, the effective use of remote sensing data depends highly on the understanding of its relation with data derived by the traditional observation methods (field data and model data). Some studies were developed within this context (Duchemin et al., 1998; Schwartz and Reed, 1999; Chen et al., 2000; Schwartz et al., 2002; Xin et al., 2002; Zhang et al., 2003; Blanch Roure, 2003; De Wit and Su, 2004), and suggested several important factors and presumptions with regard to remote sensing phenology, including: **(1)** The temporal and spatial resolution of remotely sensed data affect the accuracy of the remote sensing phenological indicators. **(2)** Surface phenology can be studied by vegetation indices (VIs), but different VIs may capture different vegetation information. **(3)** VIs are affected by a number of phenomena (comprising cloud contamination, atmospheric perturbations, variable illumination, viewing geometry), which usually reduce their values. These effects can be tackled by different methods, including data compositing and smoothing. Compositing consists of the extraction of the maximum VI value over a certain time period (e.g. one week, ten days, 16 days). This process increases the data quality, but it is expected that effects of remaining biasing phenomena persist. Smoothing algorithms and curve fitting methods can be used to address these residual effects. **(4)** Changes in surface phenology are correlated to changes in the VI time-series by estimation methods. The studies suggest that different estimation methods capture different greenness status'. **(5)** With regard to the spatial, temporal and radiometric characteristics, the MODIS sensor was found most promising for vegetation

monitoring. In addition, the MODIS VI products also showed potential for vegetation monitoring.

Blanch Roure (2003) and De Wit and Su (2004) used MODIS and SPOT Vegetation data with a spatial resolution of 1 Km for phenological monitoring in the Netherlands. Start and End of the Growing Season were derived from the Normalized Difference Vegetation Index (NDVI) and the Enhanced Vegetation Index (EVI) time series by different methodologies. The results of these studies indicated the potential of the remote sensing data for phenological monitoring. However, the resolution of 1 km is inappropriate for the Dutch land cover situation where landcover is typically fragmented into areas smaller than 1 km. To minimize the mixing of the vegetation classes, higher spatial resolution is needed (Clevers et al., 2003; Pax Lenney and Woodcock, 1997). In view of these findings the current work was accomplished as an effort to increase the understanding of the relationship between remote sensing phenology and surface phenology.

1.2 RESEARCH OBJECTIVES

The following objectives and research questions were defined for the current research.

General

To evaluate the applicability of MODIS product MOD13Q1 for phenological monitoring of different vegetation classes in the Netherlands.

Specific objectives

1. ***To estimate the remote sensing phenological indicators by different combinations of vegetation indices, smoothing methods and estimation methods***

2. ***To evaluate the influence of the pixel purity on the remote sensing phenological indicators***

3. ***To investigate the relation between remote sensing indicators and corresponding field / model indicators over the past four years***

Research questions

1. *How do the different combinations of methods affect the remote sensing phenological indicators?*

2. *How does the pixel purity affect the remote sensing phenological indicators*

3. *What is the relationship between the remote sensing indicators and the field indicators over the past 4 years and which method combination gives the best simulation for which vegetation class?*

1.3 STRUCTURE OF THIS REPORT

Chapter one of this report gives a short introduction to the study subject, the problem definition and the research objectives.

In chapter two, relevant literature regarding the study context is presented and discussed.

Chapter three describes the methodology which was used in order to achieve the research objectives.

The results are presented and discussed in chapter four, and finally conclusions and recommendations are given in chapter five and six.

2 LITERATURE REVIEW

2.1 REMOTE-SENSING PHENOLOGY

In remote sensing, phenophases can be described by changes in the vegetation cover or in the amount of green biomass or Leaf Area Index (LAI), which can be measured by Vegetation Indices (VIs). The advantages of using VIs rather than the original spectral data include the following: minimizing soil and other background effects (Appendix: Figure 8-1), reducing data dimensionality, providing a degree of standardization for comparison, and enhancing the vegetation signal (Reed et al., 1994). From the different existing VIs, the Normalized Difference Vegetation Index (NDVI) is the most commonly used index for the purpose of phenology monitoring (Justice et al., 1984; Townshend and Justice, 1986; Reed et al., 1994; Duchemin et al., 1999; Schwartz, 1999; Schwartz et al.1999; Menzel, 2000; Schwartz, 2003). However, this index has several recognized limitations, including sensitivity to atmospheric conditions, saturation of NDVI values at high LAI values, and sensitivity to soil background. Depending on the platform, changing solar zenith angle can also influence the NDVI (Xiao et al., 2002). To address these biasing phenomena many VIs were developed and compared with the NDVI. Huete et al. (1997) studied 5 different VIs: NDVI, Atmospherically Resistant Vegetation Index (ARVI), Soil Adjusted Vegetation Index (SAVI), Soil and Atmospherically Resistant Vegetation Index (SARVI) and SARVI2 (modified SARVI). The investigation was concentrated on differences and similarities in sensitivity of the VIs to vegetation conditions. According to the study results, all VIs showed a qualitative relationship to variations in vegetation. The NDVI and the ARVI were found more sensitive to red reflectances, thus, seem more suitable for studies regarding the photosynthetic capacity of vegetation cover (fPAR, percentage green cover). The other indices were found to be more responsive to variations in the near-infrared (NIR) band, thus, more sensitive to structural canopy parameters, such as leaf area index and leaf morphology. In addition, in contrast to the NDVI and ARVI, the other VIs did not saturate over forested sites. Similar findings were presented by Huete et al. (2002) and Ferreira and Huete (2004) with regard to the NDVI and the SAVI and EVI. Similar to the SAVI, the EVI was found more sensitive to the NIR reflectance. According to Huete et al. (2002), the NIR reflectances traced out the growing season dynamics fairly well, while the red band showed lower sensitivity to temporal seasonal dynamics. These trends were portrayed by the EVI and NDVI.

Peddle et al. (2001) studied the performance of ten different VIs (NDVI, SR, MSR, RDVI, WDVI, GEMI, NLI, SAVI, SAVI-1, SAVI-2 and Spectral Mixture Analysis (SMA) with regard to their capacity in providing estimates of forest biophysical information such as biomass, leaf area index (LAI) and net primary productivity (NPP). The SMA provides the capability to derive the percentage of sunlit crowns, background, and shadows within a remote sensing image pixel. This sub-pixel scale information has been shown to consistently provide significantly improved estimates of the biophysical parameters. According to their results, the SMA performed best, while the WDVI and the SAVI-1 provided the best improvement when compared to the NDVI.

2.2 DATA SMOOTHING AND DENOISING

Vegetation indices derived from satellite data may be reduced due to cloud contamination, haze, and other atmospheric effects, which can disturb the temporal profile of the vegetation signal. To eliminate these depressions, which can affect algorithms that are searching for increasing or decreasing trends representing real phenological shifts, a temporal smoothing of the data is typically performed (Schwartz, 2003). There exist several algorithms which are applicable for the smooting of VIs: BISE (Best Index Slope Extraction), Compound mean and median filter, Splines, Weighted least-squares approach (Schwartz, 2003); HANTS (Harmonic Analysis of Time Series) algorithm (Roerink et al., 2000; De Wit and Su, 2004); Savitzky-Golay based filter (Chen et al., 2004).

Reed et al. (1994) used the median filter to smoothen NDVI data and found it effective in minimizing the effects of extremely low NDVI values related to cloud contamination. However, an undesired effect of this filter is the lowering of high NDVI values which are presumed to be valid. The BISE overcomes this problem, but requires the determination of some parameters (sliding period and threshold) which highly depend on the experience and the skills of the analyst.

Roerink et al. (2000) used HANTS for the reconstruction of NDVI composites. This algorithm was developed based on the Fast Fourier Transform (FFT) with the objective to deal with time series of irregularly spaced observations (in contrast to the FFT), and to identify and remove cloud contamination observations. According to the author, the method is promising, however, the determination of two of the control parameters has no objective rules which makes the process depending on the experience of the analyst. De Wit and Su (2004) adapted the FORTRAN based method to an ENVI / IDL format and applied the modified version to NDVI data derived from the SPOT-VGT dataset. Their results were found promising for the use of HANTS for the derivation of phenological indicators in the Netherlands.

Chen et al. (2004) compared the performance of the BISE, the Fourier based fitting method (FFM) and a Savitzky – Golay filter based method (SG) on the reconstruction of NDVI time-series. According to their results, the FFM obtained the smoothest curve, but shows large displacement away from the original NDVI values (lower values). In addition, the FFM also generates spurious oscillations in the time series. In contrast to this method, the BISE and the SG obtained almost identical results. However, the SG parameters are easier to define than the BISE parameters. The determination of the treshold of the BISE involved a manual trial and error procedure to obtain the best results, while the SG parameters were set as constant combinations.

2.3 ESTIMATION OF THE PHENOLOGICAL INDICATORS

The smoothing of the VIs time series can enable a more accurate estimation of the key Remote-Sensing based Phenological Indicators (RSPIs), which are: Start of the growing season (SOS), End of the growing season (EOS) and Growing season length (GSL). The estimation of these indicators can be realized by several methods, but the most cited are described below: (1) threshold-based, (2) inflection point, (3) maximum increase and (4) delayed moving average.

(1) The threshold-based method consists of the setting of a NDVI threshold for SOS / EOS. When the NDVI value reaches this value, SOS is reached. According to Schwartz (2003), this reference value can be effective for the determination of local SOS values, with homogeneous soil background characteristics and land cover types. Reed et al.. (1994) evidenced the limitation of this method when he demonstrated that NDVI values at SOS, over the USA, might vary from 0.08 to 0.40. To overcome this problem, the Seasonal Midpoint NDVI (SMN) can be used, which ties the threshold to the seasonal amplitude of each pixel.

(2) By the inflection point method, the SOS is defined as where the time derivative transitions from 0 to a positive number (Badhwar, 1984; Moulin et al., 1997; Zhang et al., 2003). The EOS is defined as where the time derivative transitions from negative to zero. The advantage of this approach is that it permits the description of multiple growing seasons and discriminates an additional phase in the VI profile which is presumed to be related to maturity (Schwartz, 2003).

(3) The Maximum Increase approach (MI) defines the SOS where the VI data exhibit the maximum increase. Kaduk and Heimann (1996) defined the SOS as the date of the largest increase after the monthly mean temperature had reached 5^{o}. Celsius.

(4) Reed at al (1994) determined the SOS by the use of a backward-looking or Delayed Moving Average (DMA). A trend change is defined as when the NDVI values become larger than those predicted by the DMA

Schwartz and Reed (1999) accomplished a study comparing surface modelled phenology with remote sensing phenology. The authors mentioned two limiting factors for their analysis: the low temporal resolution (14-days) and the relatively invariant climate of the study period (1991-1995). The study also evidenced that for forests, the satellite sensor detects understory SOS rather than the dominant species. The same author (Schwartz et al., 2002), conducted a study concerning two SOS measures (DMA and SMN) and found that the DMA was relatively earlier than the SMN. According to the authors, DMA was detecting the first sustained flush of greenness, while the SMN was designed to predict the initial leaf expansion of the dominant overstory species.

It is clear that the different estimation approaches measure fundamentally different processes. In general, inflection point approaches will show the earliest SOS, followed in order by the DMA, MI, and at last, the SMN (Figure 2-1). The inflection points depict the time at which the VI first begins to increase, while the DMA is a more conservative measure of the increase designed to eliminate false SOS. The time

of the maximum increase is most likely when early season growth is at its peak (what a lay-person thinks of as the beginning of spring) and SMN presumably occurs when the vegetation has reached an established stage (Schwartz, 2003).

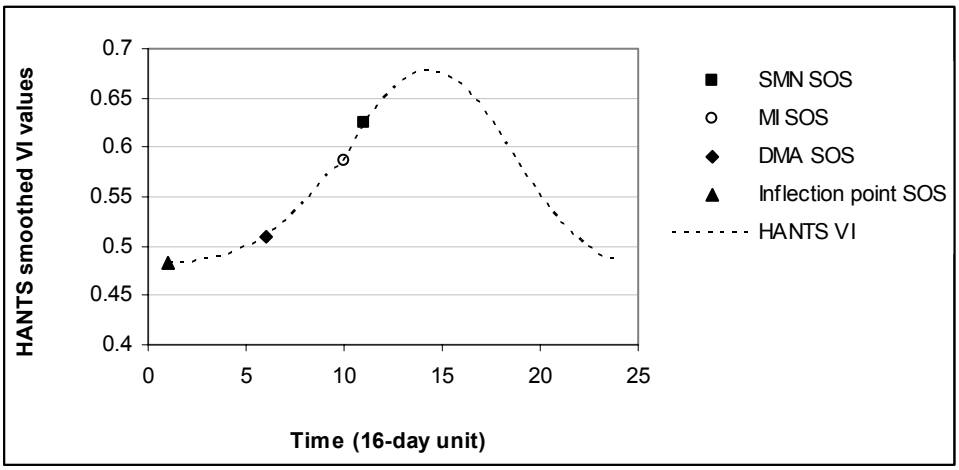

Figure 2-1. HANTS smoothed EVI time series with SOS dates according to different estimation methods.

2.4 APPLICABLE SENSORS FOR PHENOLOGICAL MONITORING

Pioneering remote sensing monitoring studies, which started in the mid 1980s used mainly images from the National Oceanic and Atmospheric Administration's (NOAA - AVHRR) advanced very high-resolution radiometer (Justice et al., 1984; Justice et al., 1986; Mauser, 1986; Townshend and Justice, 1986). Despite the advantages (mainly phenology information at global scale), the coarse resolution (1 Km) of these images limits the ability to detect important phases as budding and flowering and doesn't guarantee pure pixels. Current researches are exploring newly launched sensors and different methods for the estimation of the phenological indicators (Justice et al., 1989; Reed et al., 1994; Moulin et al., 1997; Kasischke and French, 1997; Duchemin et al., 1999; Botta et al., 2000; Zhang et al., 2002; Schwartz et al., 2002; Privette et al., 2002; Huete et al., 2002; Zhang et al., 2003; Blanch Roure, 2003; Ferreira and Huete, 2004). Among the different sensors, the MODIS (The Moderate Resolution Imaging Spectroradiometer) and the SPOT 5 VEGETATION can be considered as most suitable for the study of phenological changes. Both have an appropriate spectral, spatial and temporal resolution for the purpose of vegetation studies. However, the MODIS has free products with higher spatial resolution (250 m / 500 m). The MODIS products (NDVI, EVI, LAI, among others) have been investigated by several authors and were found superior and applicable for vegetation monitoring (Privette et al., 2002; Huete et al., 2002; Zhang et al., 2003; Blanch Roure, 2003). Huete et al. (2002) analysed the radiometric and biophysical performance of the MODIS VIs (NDVI and EVI) by studying their correlation with airborne measured top-of-canopy reflectance and field derived biophysical measures. Their results demonstrated good correspondence between the VIs and the validation data for several biomes in North and South America. According to the author, the MODIS NDVI saturated in high biomass regions, such as the Amazons, while the MODIS EVI remained sensitive to canopy variations.

Teillet et al. (1997) studied the impact of the spatial, spectral and radiometric characteristics on different VIs of a forested region. He compared VIs from different sensors (MERIS, MODIS, SPOT HRV, TM, and AVHRR) and came to the conclusion that NDVI values clearly decrease as the spectral bandwidth of the bands making up the vegetation index increases from 10 nm up to 150 nm. The decrease is more significant for spectral bands wider than 50 nm. Thus, for an optimum NDVI definition, the red spectral band should be less than 50 nm. Within this context the author classified the MERIS (10 nm) and the MODIS (50 nm) sensors as most promising for studies on vegetation indices.

2.5 RS APPROACH OF PHENOLOGICAL MONITORING IN THE NETHERLANDS

The relation between surface phenology and remote sensing phenology is affected by many factors. The literature review on this subject evidenced various, including:

- Atmosphere and ground surface factors (vegetation types, growing period, climate, pests, background, clouds, atmospheric conditions);
- Instrumental factors (view angle);
- Methodological factors (processing, smoothing and estimation methods)

To achieve the objectives of this work we designed the methodology in view of these factors for the Dutch land cover situation. To evaluate the effect of the different factors, we used fundamentally different VIs, smoothing algorithms and estimation methods.

3 MATERIALS AND METHODS

3.1 STUDY AREA

The study was realized on three vegetation classes in the Netherlands: deciduous forest, grassland and winter wheat (Figure 3-1). The decision to work with these classes was made based on the availability of the necessary input data: field data, model data, land cover data and remote sensing data. From the three classes, the grassland cover was the largest, occupying 40% of the land area of the country, followed by the wheat and forest classes with respectively 5% and 3.5% of the land area. For further analyses on the phenological monitoring, we used a smaller area representing the "pure" vegetation classes.

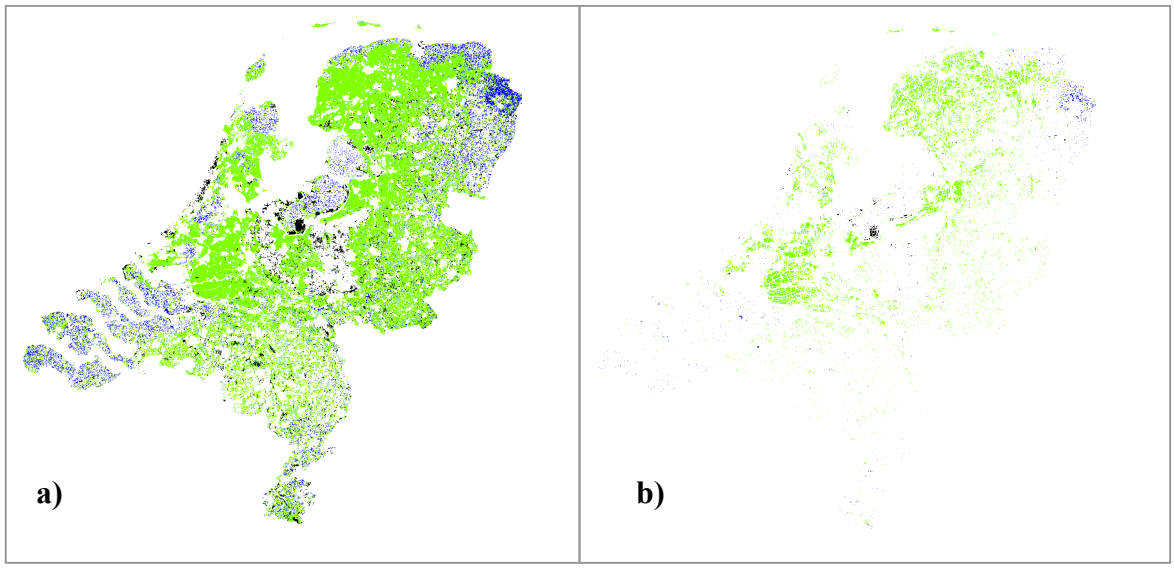

Source: LGN4 (www.alterra.wur.nl/uk/cgi/lgn)

Figure 3-1. Study area: a) The complete vegetation cover and b) "Pure" vegetation classes.

3.2 DATASETS

3.2.1 REMOTE SENSING DATA

The remote sensing data were downloaded from the MODIS gateway (EOS-MODIS, 2004). With regard to the spatial and temporal resolution, the MODIS VI product was found most suitable for the purpose of this study. Another option would be the MODIS LAI dataset, but this product was only available with a spatial resolution of 1 km.

The product we used was the MOD13Q1, from 2000 to 2004. The dataset consists of images with 16 – day NDVI and EVI composites. Each image has 11 bands containing the following information:

- ***250m 16-day NDVI***
- ***250m 16-day EVI***
- ***250m 16-day NDVI Quality***
- ***250m 16-day EVI Quality***
- 250m 16-day red reflectance
- 250m 16-day NIR reflectance
- 250m 16-day blue reflectance
- 250m 16-day MIR reflectance
- 250m 16-day average view zenith angle
- 250m 16-day average sun zenith angle
- 250m 16-day average relative azimuth angle

The two MODIS VIs complement each other in global vegetation studies and improve upon the detection of vegetation changes and extraction of canopy biophysical parameters. Whereas the NDVI is chlorophyll sensitive, the EVI is more responsive to canopy structural variations, including leaf area index (LAI), canopy type, plant physiognomy, and canopy architecture (TBRS-MODIS, 2004). The MODIS NDVI (3.1) is referred to as the "continuity index" to the existing 20+ year NOAA-AVHRR derived NDVI time series, which could be extended by MODIS data to provide a longer term data record for use in operational monitoring studies (TBRS-MODIS, 2004).

$$NDVI = \frac{\rho_{NIR} - \rho_{RED}}{\rho_{NIR} + \rho_{RED}} \qquad \textbf{(3.1)}$$

Where:

ρ_{NIR} = NIR Rflectance
ρ_{RED} = RED Rflectance

The reflectance values are the surface bidirectional reflectance factors for MODIS bands 1 (620 - 670 nm) and 2 (841 - 876 nm).

The EVI was developed to optimize the vegetation signal with improved sensitivity in high biomass regions and improved vegetation monitoring through a de-coupling of the canopy background signal and a reduction in atmosphere influences. The equation (TBRS-MODIS, 2004) takes the following form:

$$EVI = G * \frac{\rho_{NIR} - \rho_{RED}}{\rho_{NIR} + C_1 * \rho_{RED} - C_2 * \rho_{BLUE} + L} \quad \textbf{(3.2)}$$

Where:

ρ_{NIR} = NIR Reflectance
ρ_{RED} = RED Reflectance
ρ_{BLUE} = BLUE Reflectance
C_1 = Atmosphere Resistance Red Correction Coefficient (C_1=6)
C_2 = Atmosphere Resistance Red Correction Coefficient (C_2=7.5)
L = Canopy Background Brightness Correction Factor (L=1)
G = Gain factor (G = 2.5)

More details concerning the MOD13Q1 dataset can be observed in Table 3-1.

Table 3-1. Main characteristics of the MOD13Q1

Data type	16 bit signed integer
Valid range	-2000 – 10 000
Fill value	-3000
Units	NDVI / EVI
Grid	4800 x 4800
Projection type	Sinusoidal projection
File format	Hdf-eos
Image Area	Tile h18v03
File size	~ 500 MB

3.2.2 LAND COVER DATA

Land cover data were acquired from the most recent land use database of the Netherlands (LGN4), which provides data in a raster format with a cell size of 25 x 25 meters. This database has 5 superclasses (agriculture, forest, water, urban area, nature area), which are subdivided in 39 classes[2].

3.2.3 VALIDATION DATA

Field phenological indicators for forest and grassland were provided by the Natuurkalender[3] (Appendix: Table 8-1; Table 8-2;Table 8-3; Table 8-4; Table 8-5;

[2] www.alterra.wur.nl/UK/cgi/LGN (2004)
[3] www.natuurkalender.nl. (2004). Department of Environmental sciences and system analyses. Wageningen University. ATTN: of Mr. van Vliet, A. and Mr. Grutters, M.

Table 8-6). We obtained summary statistics (mean, median, min, max, n, standard deviation) of the main phenophases of forest and grassland species for the Netherlands from 2001 to 2004. The main forest species were selected based on information from the last forest inventory (Geodesk – CGI[4]): *Quercus robur & rubra* (Respectively: Pedunculate Oak or Zomer Eik & Red Oak or Amerikaanse Eik), *Fagus sylvatica* (Beuk or Beech) and the *Betula pendula* (Berk or Silver Birch). In addition, we also also selected data related to understory forest species[5]: *Corylus avellana* (Hazel or Hazelaar), *Crataegus monogyna* / *Crataegus sp.* (Meidoorn or Hawthorn), *Sorbus aucuparia* (Lijsterbes), *Sambucus nigra* (Vlier). For the main forest species there were data available about the phenophases: Leaf unfolding (UL), the Leaf fall (FL), Colouring 50 and 100% (CL50; CL100) and flowering (F). For the understory species only flowering (F) dates were available.

The grassland cover was represented by species as suggested by the Natuurkalender: *Cerastium arvense, Cytisus scoparius, Laburnum anagyroides, Glechoma hederacea, Alliaria petiolata, Filipendula ulmaria, Cardamine pratensis, Anthriscus sylvestris, Lythrum salicaria, Lychnis flos-cuculi, Leucanthemum vulgaris, Daucus carota, Tussilago farfara, Lamium album, Ranunculus acris, Ranunculus ficaria, Tanacetum vulgare, Caltha palustris, Ranunculus repens, Galanthus nivalis, Viola odorata.* The available phenological data consisted of flowering dates (F).

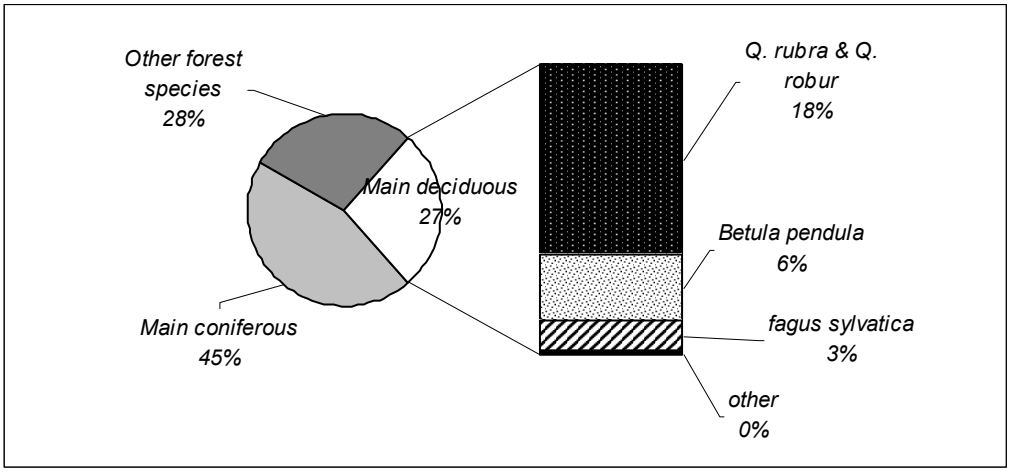

Figure 3-2. Overview of the forest composition in the Netherlands (in % of total forest area)[9]

The phenological indicators for the winter wheat were obtained from the WOFOST / CGMS model (World Food Studies / Crop Growth Simulation System [6]). This model describes phenological development, growth and yield formation of a crop from emergence till maturity on the basis of crop genetic properties and environmental conditions. For the purpose of this study we used the LAI from the model output (Appendix: Figure 8-2).

[4] Expertisecentrum LNV. Ministerie van Landbouw, Natuurbeheer en Visserij. Wageningen (2001). J. Clement, 2001. GISBOS Vierde Bosstatistiek. Wageningen, Alterra, Research Instituut voor de Groene Ruimte.

[5] http://www.bomengids.nl/hoofdsleutel.html, 09.2004

[6] http://www.supit.cistron.nl/start.htm, 01.2005

3.3 METHODOLOGY

The main goal of the present study was to investigate the applicability of MODIS data for phenological monitoring of different vegetation classes in the Netherlands. From the literature study it became clear that remote sensing phenology incorporates effects of different biasing phenomena. To assess the magnitude of these effects we decided to evaluate different methods based on combinations of (assumed) fundamentally different VIs (EVI vs. NDVI), smoothing methods (HANTS vs. SG) and estimation methods (SMN vs. MI). The applicability of the MODIS data was assessed by evaluating its capability in providing consistent information about the growing season trend and its variability over the years. The reliability of the remote sensing data was defined in relation to field and model data. Changes in the trend of the mean SOS dates can be related to ecological changes (climate, temperature). On the other hand, the changes in the variability may signal changes at the sub pixel level.

The general methodology was divided in three phases: preparation, processing and analysis (Figure 3-3). In the preparation phase we defined and prepared al necessary input data. The processing phase (Figure 3-4) involved the processing of the remote sensing data, land cover data and model data for the estimation of the phenological indicators. Five main processing blocks were necessary in this phase: (1) preparation of the input data (modis data and land cover data) for the smoothing methods; (2) parameterization of the smoothing methods; (3) smoothing of the VI time series; (4) estimation of the remote sensing phenological indicators, and finally (5) creation and application of vegetation masks to assess the effect of the pixel purity on the RSPIs.

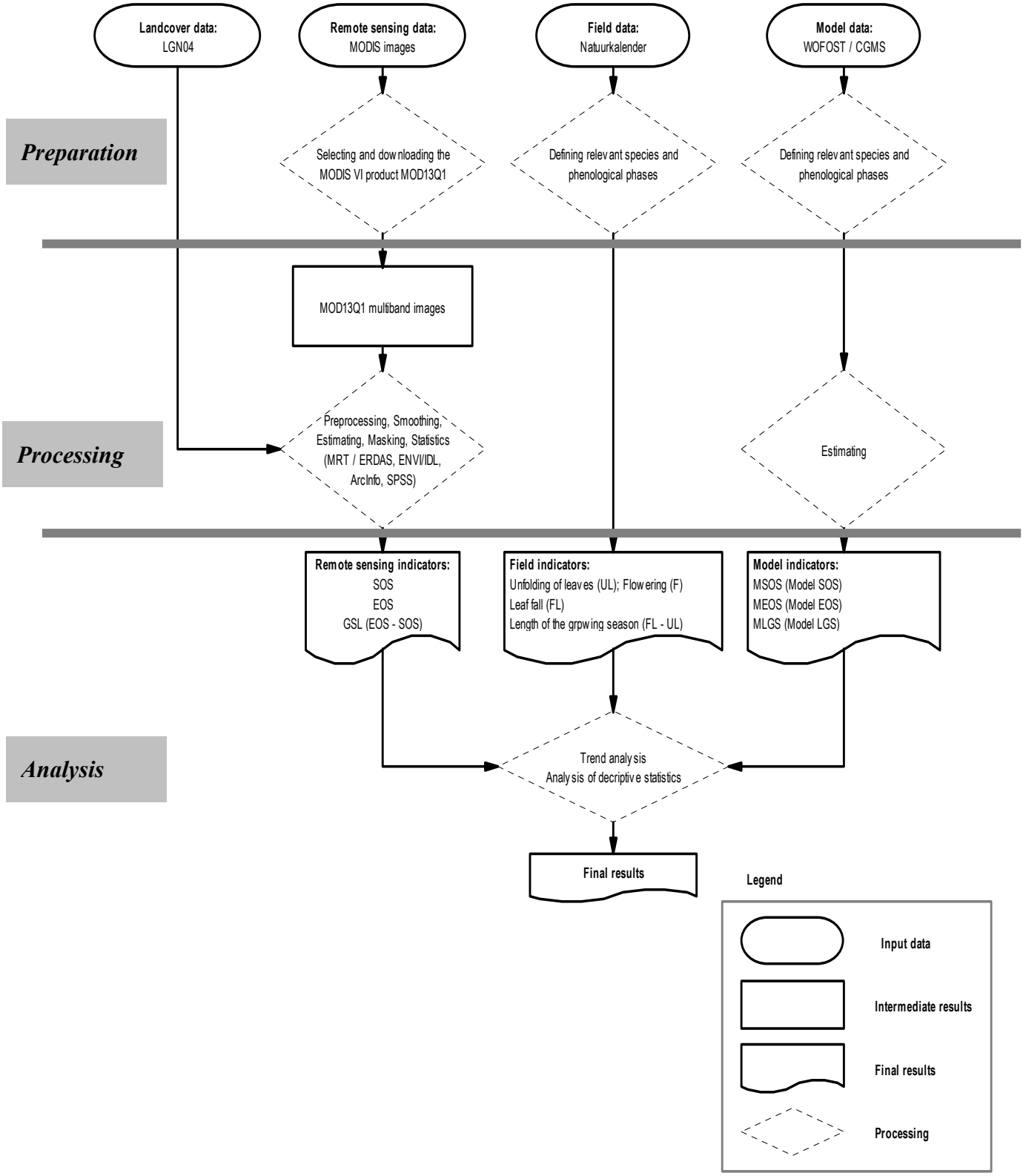

Figure 3-3. Overview of the general methodology steps

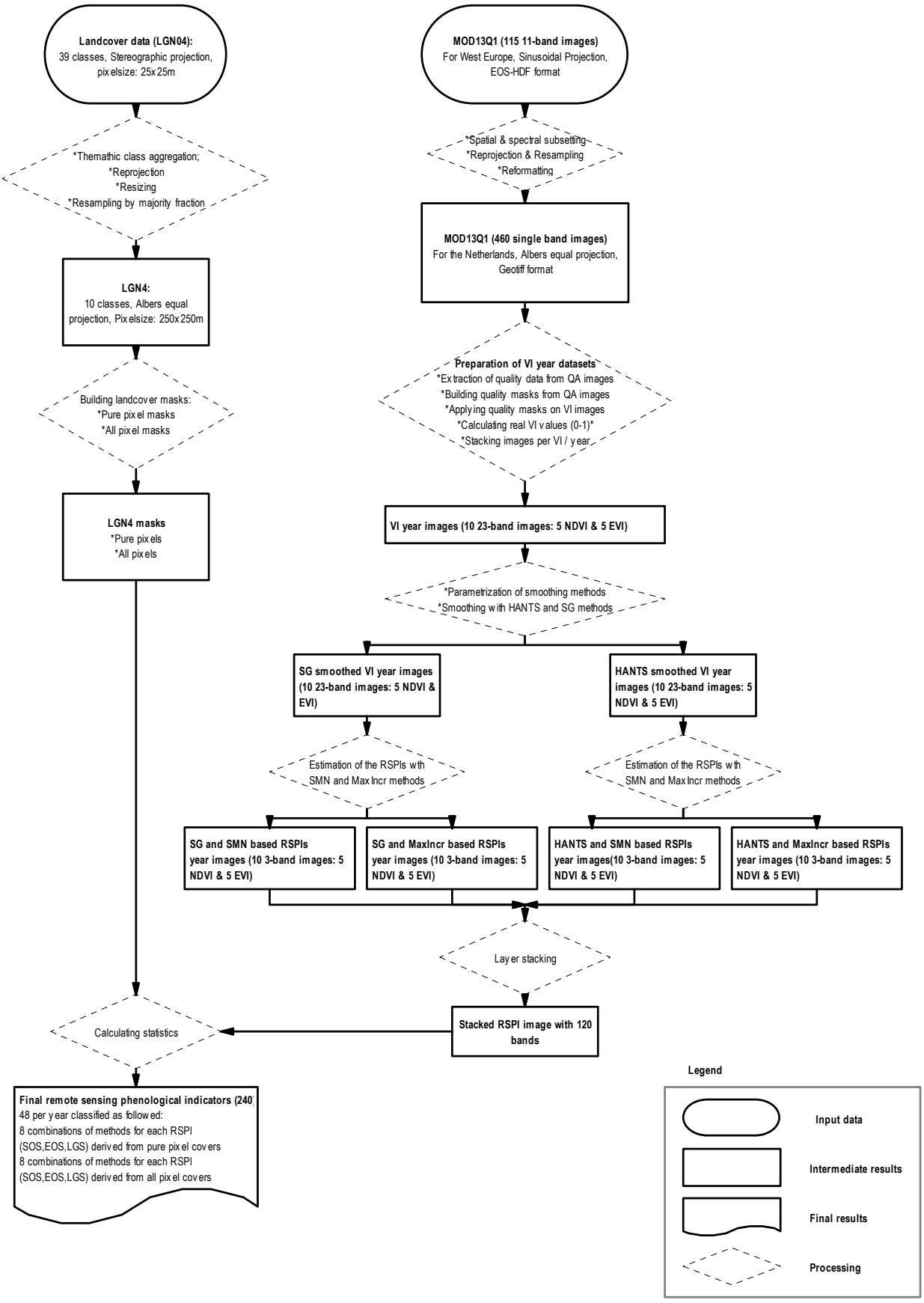

Figure 3-4. Overview of processing methodology of the LGN4 and MODIS data

3.3.1 PROCESSING REMOTE SENSING DATA

In total 112 images were downloaded from the MODIS gateway (corresponding to the period 2000 - 2004). These images were not readily useable for further analyses purposes. Therefore, to enable the extraction of the RSPIs, some preprocessing was necessary.

The first processing block was to filter the necessary data and to enable the use of the raw MODIS data within the available commercial softwares (ERDAS imagine and ENVI / IDL). The following parameters were set in the Modis Reprojection Tool (MRT) and were applied by batch processing on the 115 images:

❖ **Spatial subsetting**

Spatial subsetting was necessary to scale down the image tile (which was mainly covering the Netherlands, Germany & Belgium) to the Netherlands only (UL corner = (-1340000, 442500) and LR = (-915000, -24000)). This resulted in images with 1700 samples and 1866 lines.

❖ **Spectral subsetting**

Within the study context, we only needed information about the VIs and their quality, hence, by this parameter setting we extracted four bands of each image (NDVI, EVI, Quality data NDVI & Quality data EVI).

❖ **Reprojecting, resampling and reformatting**

Finally, the images were reprojected from the sinusoidal projection to the Albers equal projection and resampled by the nearest neighbour method. The file format was also transformed from the HDF – EOS format to the GeoTIFF format.

The second processing block was realized to extract quality information from the Quality Assessment images of both VIs (Appendix: Table 8-8). This information was used to create quality masks for the VI images. Processing was done by batch processing in IDL / ENVI:

❖ **Extraction of the quality bits**

The quality control bits of this dataset were at positions 10, 11, 12 and 13 of each pixel. Since we were only interested in these specific bits, we first set al other bits to '0' by applying a bitwise AND operation to each pixel:

R1 = D AND 15360 (This function extracts only the bits at the positions 10, 11, 12 and 13).
R2 = R1 / 1024 (with this function, we shift the bits 10 positions to the right, in order to have them on positions 0,1,2 and 3).
Where: D = Input QA image; R1 = Output image with only the quality bits at the positions 10, 11, 12 and 13; 15360 = binary number 0011110000000000; R2 = Output image with the quality information now on positions 0,1,2 and 3

❖ **Building and applying quality masks**

The previous step gave origin to images with only information about the quality level of each pixel. The values were ranging from 0 to 15 (corresponding to the binary numbers 0000 up to 1111), from perfect to non – useful. We used the interval [0,6], from *perfect* to b*elow intermediate quality* but above *average quality*. The quality masks were built by giving 1 to all pixels with the value within the defined interval. All the other pixels got the value 0. The masks were applied on the VI images and the masked images were stacked per VI for each year. The final images were in the Envi file format, albers equal projection, Float datatype, and were screened for low quality pixels.

3.3.2 SMOOTHING METHODS

For the smoothing step, we decided to work with the HANTS algorithm as described by De Wit and Su (2004) and the Savitzky Golay based method as presented by Chen et al. (2004). The first mentioned method is appeared to be a robust and fast smoother, while the second one was found to be very precise in following the VI curve (Figure 3-5). The HANTS algorithm assumes that vegetation development, as indicated by VIs, has a strong seasonal effect (in most parts of the world, apart from the tropics) which can be described using a series of low frequency sine functions with different phases, frequencies and amplitudes. Disturbing effects are usually more or less randomly occurring spikes in the VI time-series and can be considered as high frequency "noise". This algorithm is based on a Fourier analysis (De Wit, 2004). The SG method is based on two similar assumptions: (1) VI data from satellite sensors are primarily related to vegetation changes. Thus, a VI time-series follows annual cycle of growth and decline; and that (2) clouds and poor atmospheric conditions usually depress VI values, requiring that sudden drops in the VI time – series, which are not compatible with the gradual process of vegetation change, be regarded as noise and removed. The SG method is a simplified least-squ

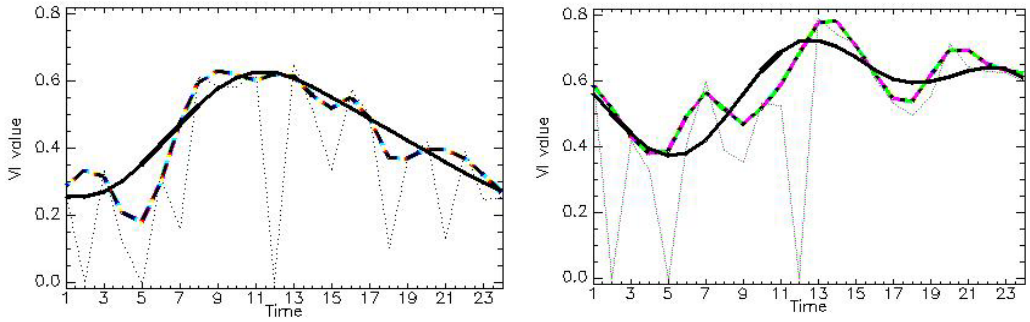

Figure 3-5. Illustration of the smoothed EVI time series of two single random pixels.
Dotted line is the original EVI data, solid line is the HANTS smoothed data and the dashed line is the SG smoothed EVI data.

❖ Parameterization of the HANTS method

The HANTS smoothing method (Figure 3-6) uses the stacked VI time-series as input and has five parameters to be set: RANGE, FREQS, IMAX, FET and TAT. The first two parameters are defined by the characteristics of the input dataset and the analysis period. RANGE refers to the valid VI range, in our case [0,1]. FREQS refers to the frequencies to be selected from the fourier spectrum. In our case, we used FREQS = [0,1,2], where 0 refers to the mean; 1 and 2 refer to the sine waves 1 and 2.

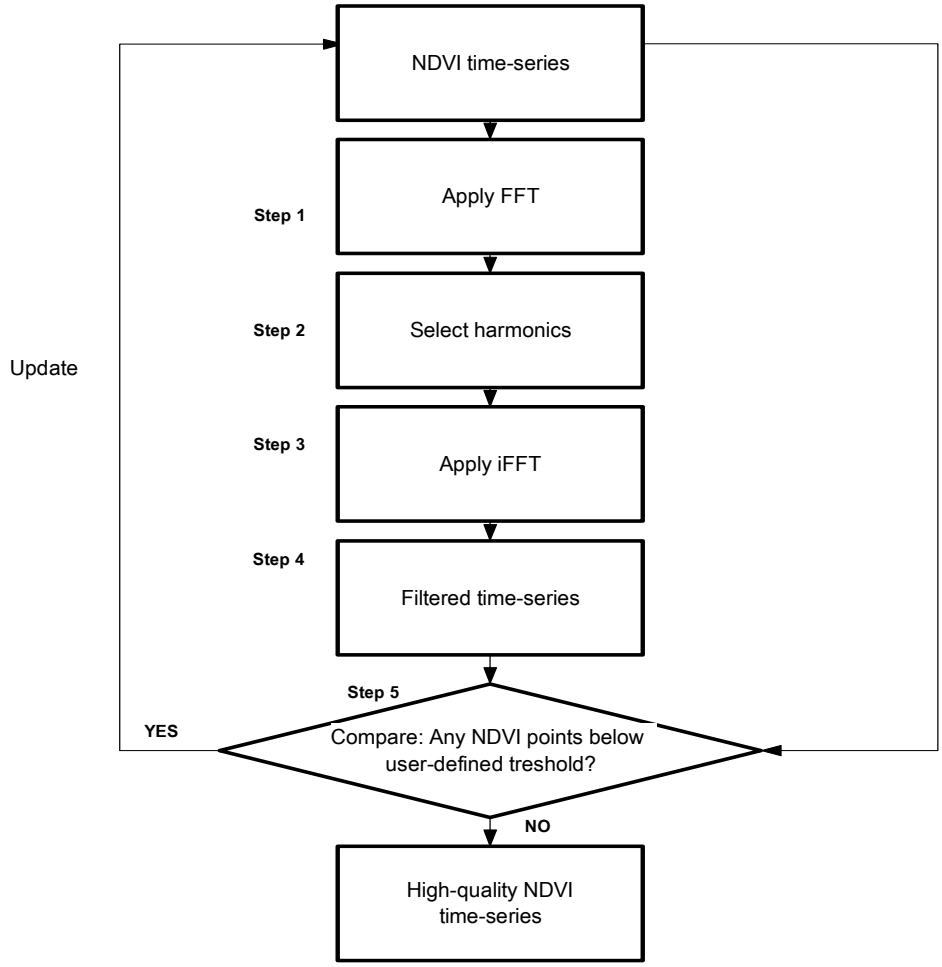

Figure 3-6. Flowchart of the HANTS smoothing method adapted from De Wit and Su (2003).

The HANTS smoothing method consists of two main iteration loops. The first loop is to find corrupted data points and to substitute them by the FFT smoothed data. This loop is the most important loop and is controlled by the parameters FET (determines the corrupted points), TAT (determines the maximum number of loops) and IMAX (controls never-ending-loops). The second loop is to stabilize the profile, by updating the previously detected corrupted points by FFT smoothed data. This iteration process is controlled by IMAX and the mean VI value.

The more crucial parameter to determine was the FET. As it concerns the maximum deviation allowed between the smoothed curve and the original data, it was necessary to evaluate the variation of the VI curves over the years to get an indication about its deviation range (Figure 3-7).

For the determination of this parameter, we used bands 6 up to 20 of the stacked real value EVI & NDVI images, considering them as generally representative bands for the growing season in the Netherlands. The standard deviation per band number over year 2000 to 2004 was calculated on a pixel basis, which resulted in an image with standard deviation values of the respective band over the four years. The resulting images were stacked into one image and the mean standard deviation per pixel was calculated. This step resulted in an image containing the mean standard deviation values over all bands.

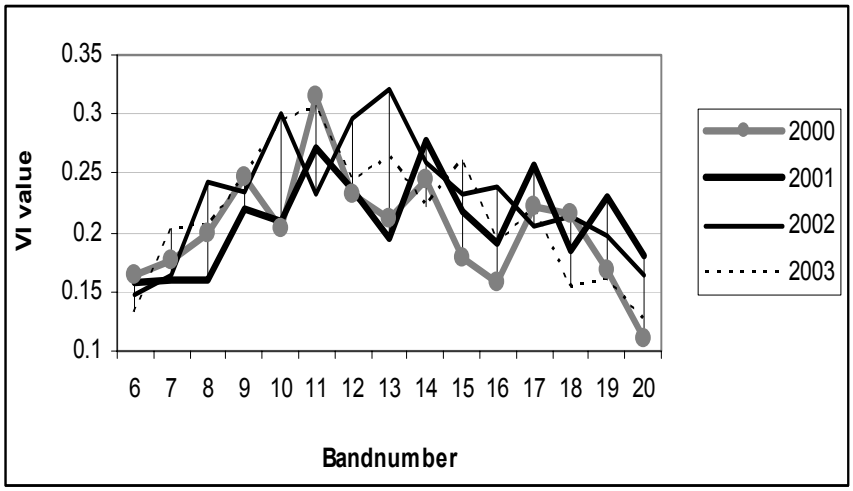

Figure 3-7. Example of the procedure for the determination of the FET on a single random pixel.

The summary statistics of the calculated standard deviations can be observed in Table 3-2. Based on these results, we decided to use the value 0.1 for the FET parameter. The last parameter, TAT, refers to the maximum number of points which can be eliminated in the smoothing process. The TAT value was set as 1/3 of the number of points within the VI profile.

Table 3-2. Summary statistics for the standard deviation of EVI and NDVI values, calculated over bands 6 to 20, over the years 2000 to 2004

VI	Mean	St.Dev	Min	Max	N
EVI	0.111330	0.033956	0	0.338234	2020578
NDVI	0.133252	0.042061	0	0.403978	2020578

Finally, the parameters were set as followed: RANGE [0,1]; FREQS [0,1,2]; IMAX = 10; TAT = 8; FET = 0.1. The results were evaluated by visual analysis and were found satisfactory (Figure 3-8).

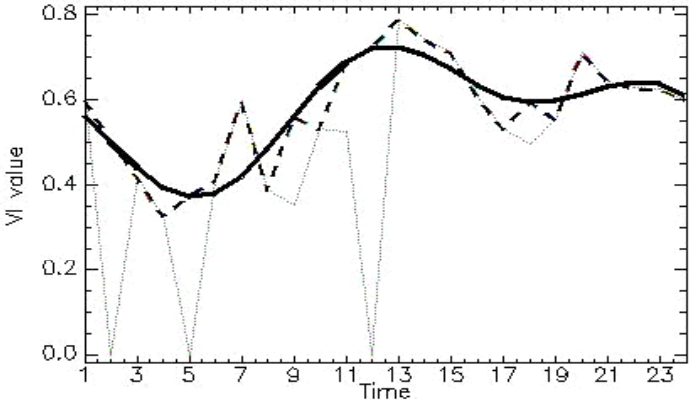

Figure 3-8. Illustration of the HANTS smoothed EVI time series of a single random pixel
Dotted line is the original EVI data, dashed line is the interpolated EVI data, solid line is the HANTS smoothed EVI data.

❖ Parameterization of the Savitzky – Golay based method

The Savitzky-Golay based method (SG) (Figure 3-9) uses the stacked VI images, stacked quality assessment images and a land – water mask as input. Two parameters are required to be set for this method. The first is the half width of the smoothing window, m. The second parameter is the degree of the smoothing polynomial, d, which typically is set in a range from 2 to 4. A smaller value will produce a smoother result but may introduce bias; a higher value will reduce the bias, but may "overfit" the data and give a noisier result.

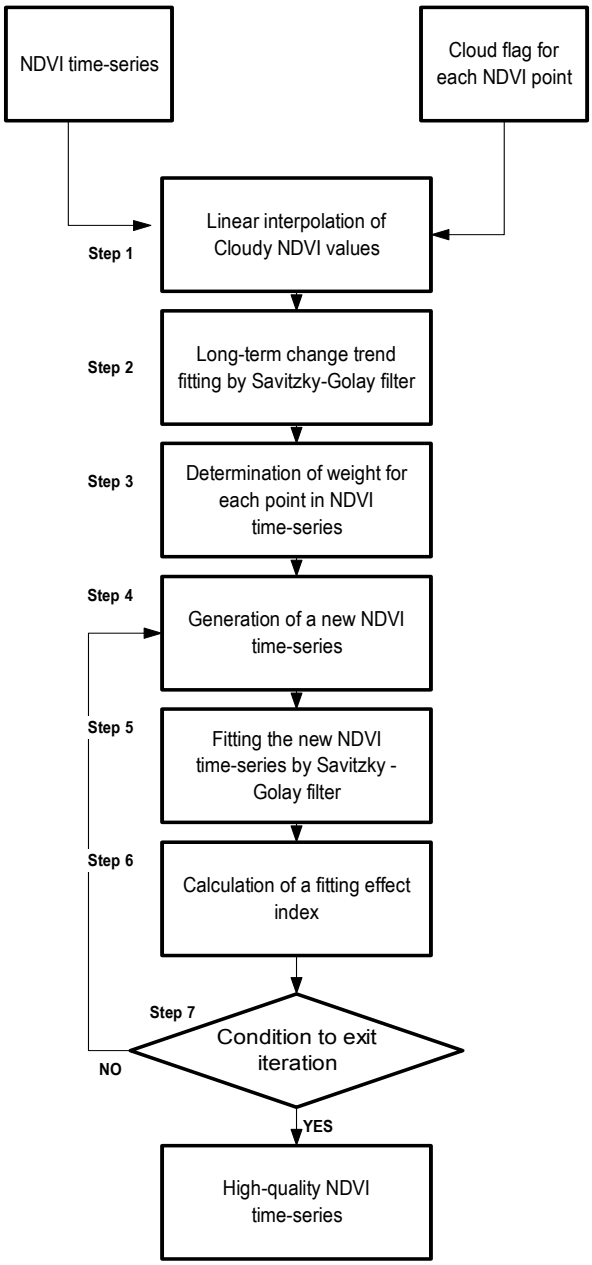

Figure 3-9. Flowchart of the Savitzky Golay based smoothing method adapted from Chen et al.. (2004)

Chen et al. (2004) evaluated several combinations of the two parameters and suggested the combination (m,d) = (3,4) as the optimal combination. According to the authors, the parameter combination is robust and can be applied to datasets at different intervals, such as daily data, 10-day data, or monthly data. We tested several other combinations in addition to the suggested combination. From a qualitative analysis of the results, the suggested parameter combination was found to perform best (Figure 3-10). Hence, we used the suggested combination for the present study.

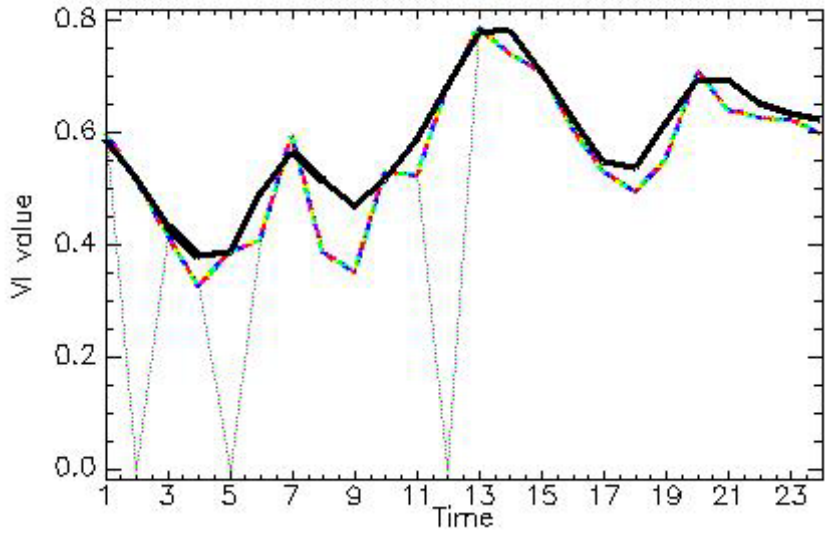

Figure 3-10. Illustration of the SG smoothed EVI time series of a single random pixel
Dotted line is the original EVI data, dashed line is the interpolated EVI data, solid line is the SG smoothed EVI data.

3.3.3 ESTIMATION OF THE REMOTE SENSING PHENOLOGICAL INDICATORS

The remote sensing phenological indicators were estimated by two methods (Figure 3-11): the Threshold based Seasonal midpoint VI (SMN) approach as described by White et al. (2002) and the Maximum increase increase (MI) in VI as presented by Kaduk and Heiman (1996) and De Wit and Su (2004). None of the two used methods consider multiple growing seasons, but this situation was not expected for the studied vegetation classes.

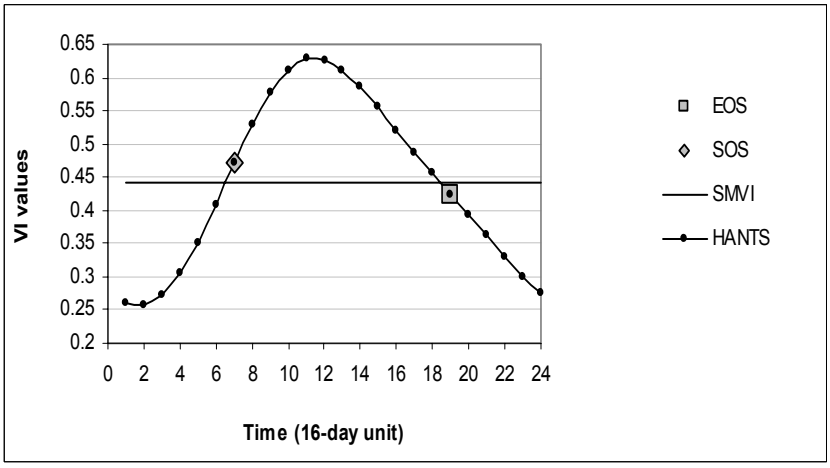

SMN: On a pixel basis, the maximum and minimum of the VI curve were derived per year. Then the mean of the two points was calculated (SMVI). For each pixel, the SOS was defined as the time unit greater than or equal to the time unit at the SMVI. The EOS was defined as the time unit at the first VI value smaller than the SMVI.

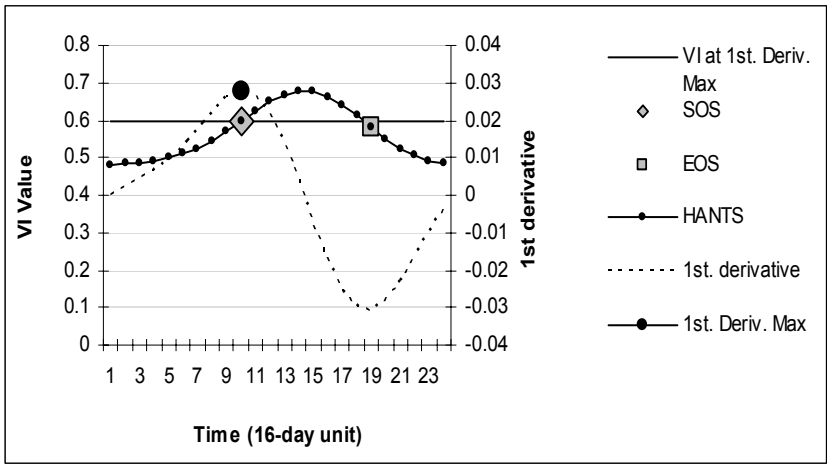

MI: On a pixel basis, the first derivative of the VI curve was defined. The SOS was defined as the time unit of the VI with the maximum increase. The EOS was defined as the time unit at the first VI value smaller than the VI at maximum increase.

Figure 3-11. Illustration of the estimation of the SOS and EOS by the SMN and MI methods.

3.3.4 CREATING LAND COVER MASKS

The LGN4 database was used to create vegetation masks. To enable masking of the remote sensing images, both datasets needed to be in the same format (pixel size, projection). Hence, the following preprocessing steps were realized on the LGN4 image:

❖ **Thematic class aggregation / recoding**

The 39 classes of the LGN4 were aggregated into 10 classes within ERDAS Imagine (Table 8-7).

❖ **Reprojection and resampling**

The LGN4 geodatabase was in the Stereographic projection and was reprojected to the same projection type as the MODIS data, the Albers equal area projection. Resampling was done by the nearest neighbourhood method.

❖ **Reformatting pixel size and resampling by majority fraction**

By use of the ERDAS modeller we reformatted the pixel size from 25 x 25 m to 250 x 250 m. Resampling was done by majority fraction. By doing so, it was possible to extract pixels with a purity of 100% for each vegetation class

Table 3-3. Summary statistics on the masks for each phenological class.

Phenological / LGN classes	No. of all 250 m pixels	Purity (%)	No. of pure 250 m pixels
Grassland	221,003	Mean = 77.5 Range = 18 - 100	40,333
Deciduous forest	19,318	Mean = 63.3 Range = 22 – 100	979
Wheat	29,050	Mean = 63.7 Range = 22 - 100	1,273

The resulting LGN4 was in Binary format, with a pixel size of 250 m x 250 m, in the Albers Equal projection, and with 10 main classes.

From this image, two types of vegetation masks were built:

- Masks built on all pixels for each vegetation class – “all pixel masks”
- Masks built on only 100% pure pixels – “pure pixel masks”

For the statistical analysis, the two types of masks were applied on the images with the RSPIs and this resulted in a set of 16 images per vegetation class per year, corresponding to the different methods. Each image consisted of three bands, corresponding to the phenological indicators: SOS, EOS and GSL. A general overview of the different methods can be observed in Table 3-4.

Table 3-4. Overview of the different method combinations

ndvi_sg_smn	NSS
ndvi_hants_smn	NHS
ndvi_sg_deriv	NSD
ndvi_hants_deriv	NHD
evi_sg_smn	ESS
evi_hants_smn	EHS
evi_sg_deriv	ESD
evi_hants_deriv	EHD

3.3.5 ESTIMATION OF THE MODEL INDICATORS

We obtained model LAI data from three winter wheat production areas (north-east, centre, and south-west) from 2000 to 2004. The model indicators were determined by applying the previously mentioned MI method on the LAI curves (Appendix: Figure 8-2).

3.4 ANALYSIS

The remote sensing based phenological indicators (RSPIs) were calculated per pixel and summarized per land cover type for each year. To minimize the effect of outliers on the statistics, we used a threshold for the growing season going from DOY 49 to DOY 365, based on the months with a mean temperature greater than 5^0C (KNMI). The summary statistics per vegetation class included: mean, standard deviation, minimum, and maximum. For comparison of the variability of the datasets, we used the Coefficient of Variation (3.3).

$$CV = (S / \overline{X}) * 100 \qquad \textbf{(3.3)}$$

Where: CV = Coefficient of Variance
S = standard deviation
$\overline{X}$ = mean

The effect of the different methods on the RSPIs was assessed by analysing the mean values and their trend over the four years. This analysis evidenced the differences/similarities and their magnitude between the methods over the years.

The relationship between the remote sensing data and the validation data was measured by the trend analysis of the mean and its variability. The analysis was focussed on the consistency of the differences between RSPIs and validation data over the four years.

For the forest cover, we obtained data from the different phenophases, however, for the FL, there were not enough data for accurate statistical interpretation. Hence, we focussed our analysis mostly on the SOS dates and the UL and F dates and their variability. For grassland, we compared the RS SOS means and their variability with the flowering dates and their variability. With regard to the Winter wheat, we analysed the mean SOS, EOS and GSL dates, but due to the number of samples, we did not analyze the variability of this class. All these analyses were accomplished on the " pure" vegetation classes. For the evaluation of the effect of the pixel purity on the RSPIs, we compared the mean and the CV of the two types of datasets ("pure_pixel_images" vs. "all_pixel_images"). The trend of the mean values was compared over the years, while the fit of the CV trends was assessed by the sum of squares of the differences between similar CV trends. By doing so it was possible to tell whether non pure vegetation pixels could also provide useful phenological information.

4 RESULTS AND DISCUSSION

4.1 VEGETATION INDICES

It is assumed that photosynthetic activity in deciduous forests depends on the photoperiod, moisture and temperature with specific adaptations ranging between species. A typical pattern of this activity is a winter minimum followed by a rapid increase to a maximum by late spring, persisting for 2 or 3 months, then decreasing steadily until defoliation in autumn (Reed, 1994). In general this pattern can be applied to other vegetation classes with behold of specific characteristics. Grasslands have a more extended and less clearly defined growing season than forests, while wheat has a shorter growing season than the other classes. Both VIs succeeded in giving the general long term phenological trend of the different vegetation classes, within different ranges (NDVI higher than EVI) (Figure 4-1).

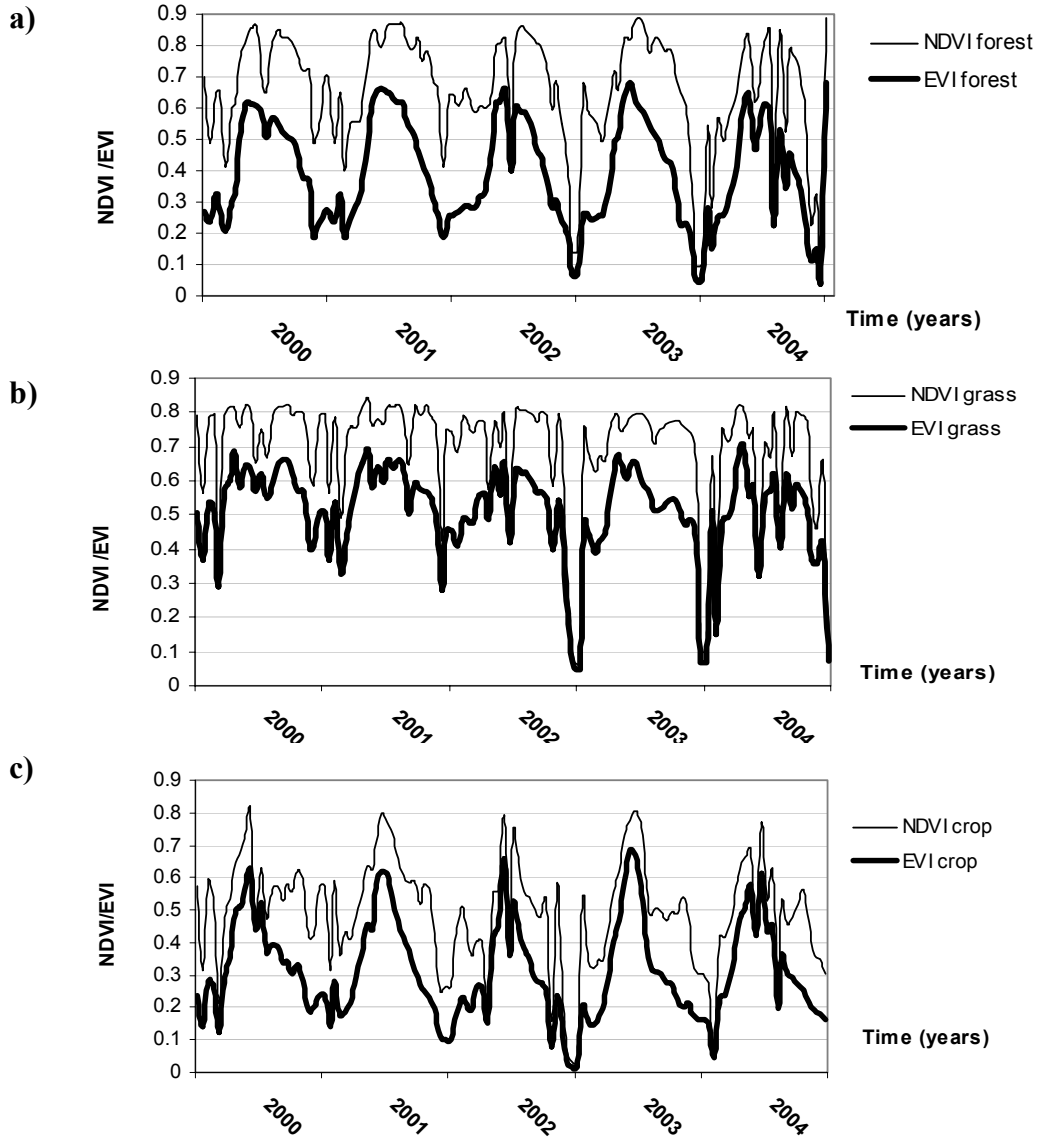

Figure 4-1. Mean original NDVI and EVI time series from 2000 to 2004 for a) deciduous forest, b) grassland and c) winter wheat

4.2 SMOOTHING OF THE VEGETATION CURVES

The two smoothing algorithms were found to perform well in a complementing way. The HANTS smoothed data followed the more general trend of the land cover, while the SG smoothed data followed the original data precisely, especially with regard to the maxima and their locations (Figure 4-2, Figure 4-3). The precision of the SG method implied some difficulties for the derivation of the RSPIs. In some cases (Figure 4-2, Figure 4-3), the original VI values demonstrate a peak immediately at the beginning of the year. This might result in a false SOS when estimated by the Maximum increase method. To minimize this problem, the statistical analysis was realized on a subset (growing season threshold) as mentioned in the methodology.

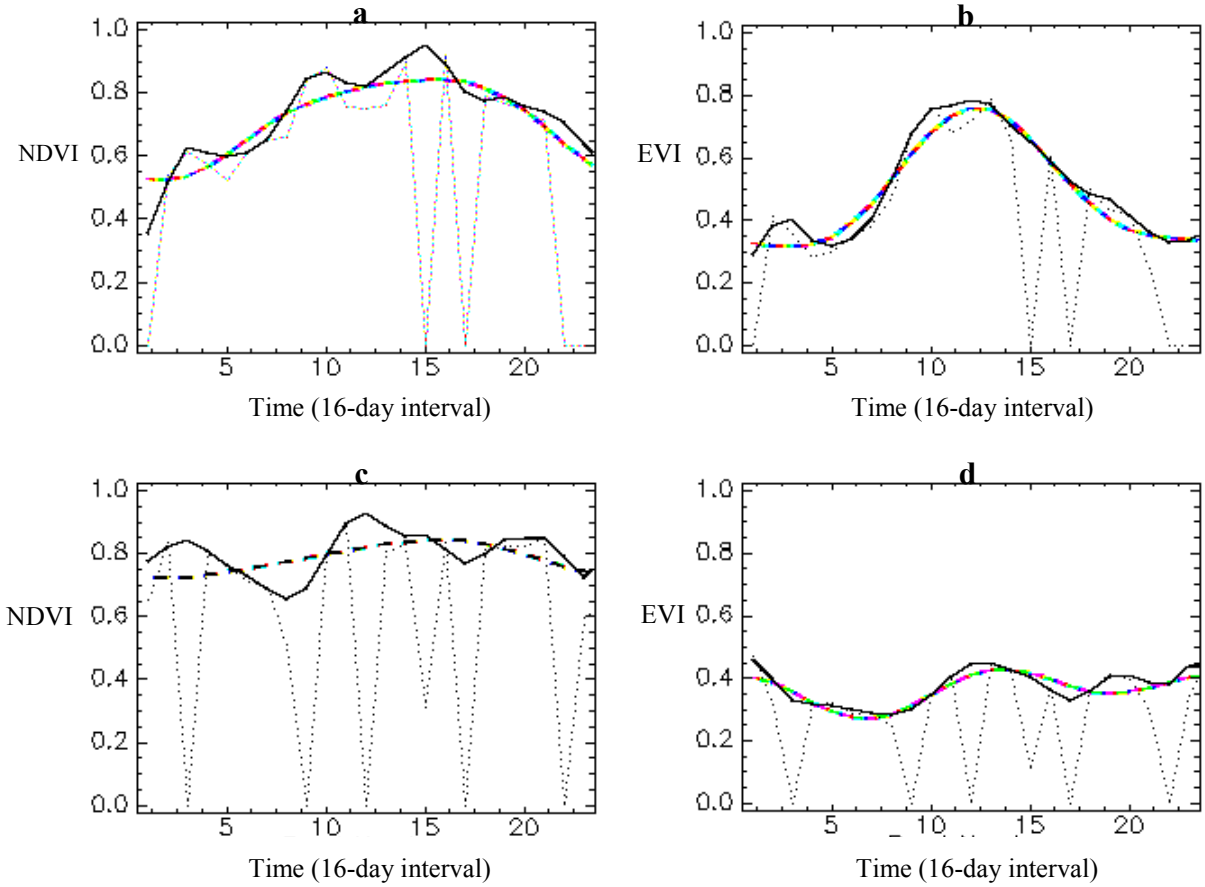

Figure 4-2. Smoothed NDVI and EVI time series (2004) for single pixels of deciduous forest (a,b) and coniferous forest (c,d)
Legend: Dotted line is the original vegetation curve. Dashed line is the HANTS smoothed curve and Bold line is the SG smoothed curve.

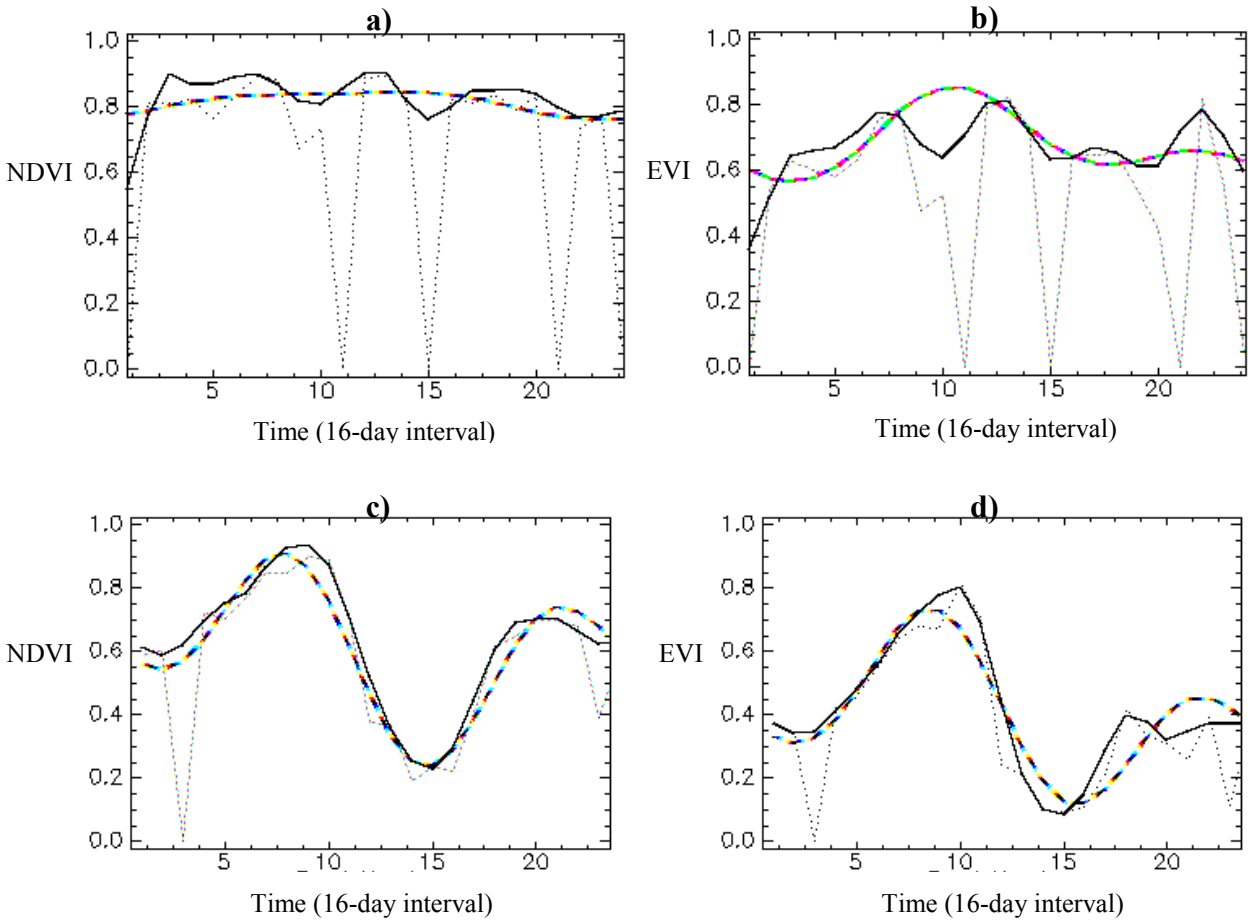

Figure 4-3. Smoothed NDVI and EVI time series (2004) of single pixels from a grassland area (a, b) and a wheat area (c, d).
Legend: Dotted line is the original vegetation curve. Dashed line is the HANTS smoothed curve and Bold line is the SG smoothed curve.

4.3 ESTIMATION OF THE REMOTE SENSING INDICATORS

❖ **Analysis of RSPIs derived from "pure" vegetation classes**

For forest and winter wheat, the supposition about the two methods, with regard to the SOS, remains valid (SMN SOS occurs later than MI SOS). For grassland, SMN SOS occurred mostly earlier than the MI SOS (Figure 4-4). Further analysis showed that the earliest SMN SOS dates were the ones derived from the NDVI time-series. This could indicate the difficulty of the NDVI in measuring small variabilities, in contrast to the EVI. The RSPIs which were derived by the ***evi_hants_smn*** and ***the evi_hants_deriv*** showed exactly similar trends for some of the indicators (forest SOS, EOS and GSL; Grass SOS, EOS and GSL; Crop EOS and GSL).

When analyzing the effect of the vegetation indices on the estimated RSPIs, we observed that the NDVI based RSPIs were mostly greater than or equal to the corresponding EVI based indicators (Figure 4-4). Grassland showed higher differences for all indicators. This could be attributed to the unclearly defined growing season of this class, which probably evidences the differences in information acquirement of the two VIs. In general, no systematic differences were observed for any of the indicators over the five years. This could be an indication of the extent of difference between the two VI algorithms.

The analysis of the smoothing methods showed that in most cases SG SOS dates were either equal to or later than the HANTS SOS dates (Figure 4-4). This was observed for all vegetation classes. In general, the SG EOS dates were earlier than or equal to the HANTS dates. No systematic differences were observed for any of the indicators over the four years.

An overview of all results can be observed in the Appendix: Table 8-9, Table 8-10 & Table 8-11).

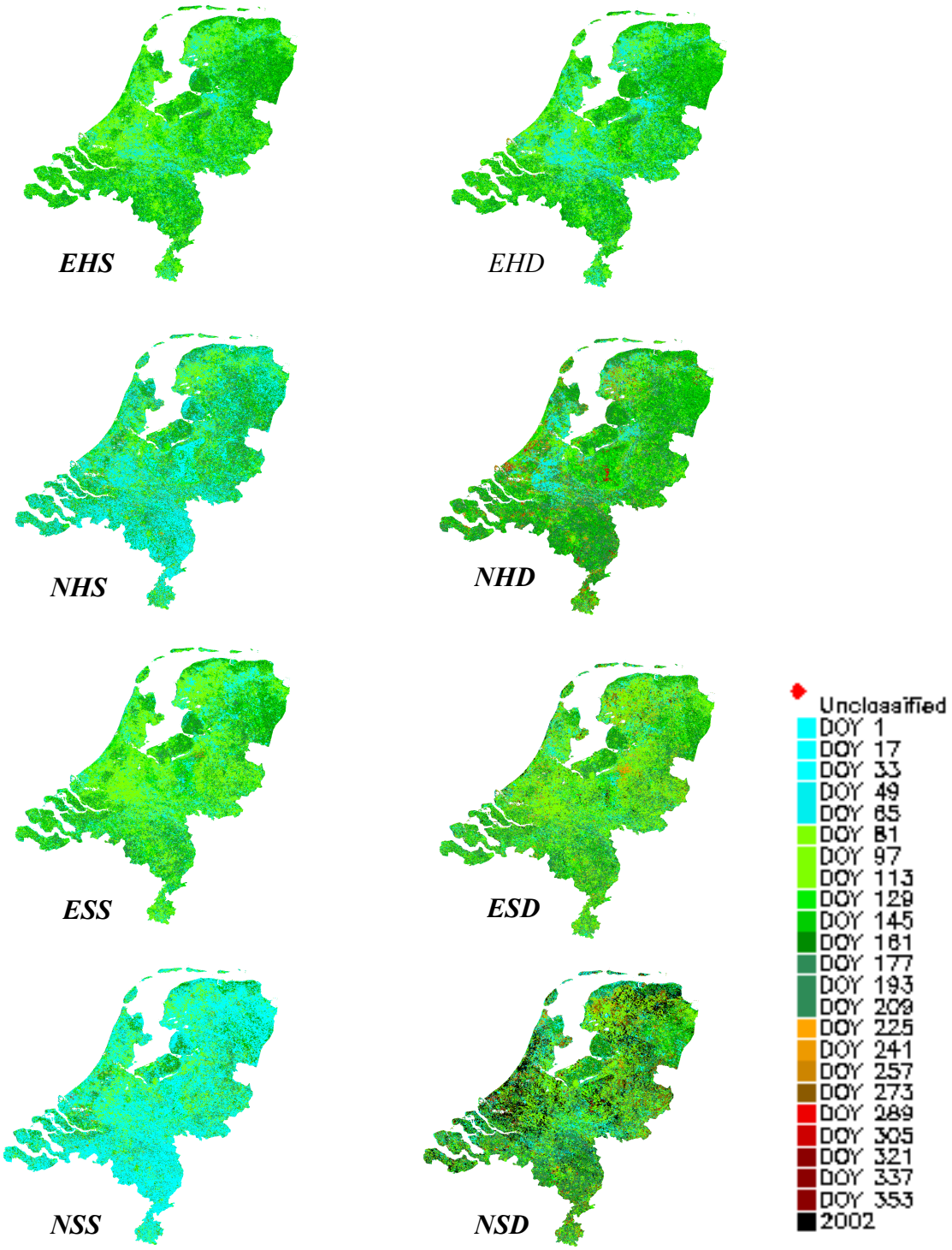

Figure 4-4 .SOS maps for 2001 according to the 8 different methods

EHS = EVI_HANTS_SMN; **EHD** = EVI_HANTS_DERIV;
NHS = NDVI_HANTS_SMN; **NHD** = NDVI_HANTS_DERIV;
ESS = EVI_SG_SMN; **ESD** = EVI_SG_DERIV;
NSS = NDVI_SG_SMN; **NSD** = NDVI_SG_DERIV

❖ Analysis of the effect of pixel purity on the RSPIs

The analysis of the effect of the pixel purity on the RSPIs, did not evidence overall similarity between the two types of vegetation cover ("pure" vegetation classes and "complete" vegetation classes). Some specific trends were observed for the five years. For grassland, SOS dates from both datasets were found similar when computed by the method ***evi_hants_smn***. The ***evi_sg_smn*** method seems to give similar information on EOS dates for the wheat and the ***evi_hants_deriv*** for the GSL dates of wheat (Figure 4-5).

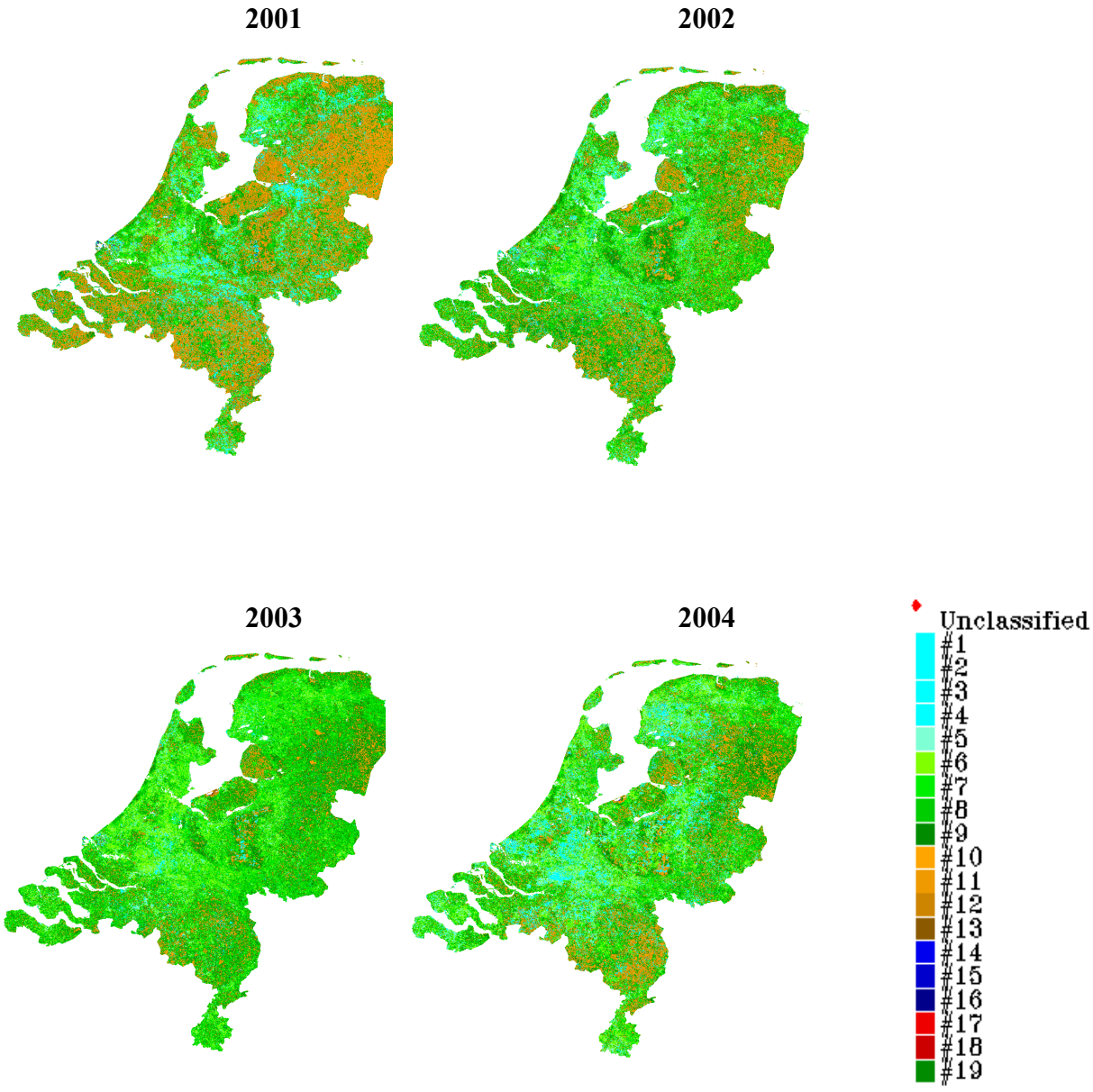

Figure 4-5. SOS maps from 2001 to 2004 according to the method combination: evi_hants_smn

Units in the legend are 16d intervals

4.4 ANALYSIS OF THE REMOTE SENSING INDICATORS: DECIDUOUS FOREST

4.4.1 FIELD PHENOLOGICAL INDICATORS

❖ Leaf unfolding (UL)

According to the Natuurkalender, leaf unfolding of the main forest species, with exception of the *Quercus robur*, occurred in the month April (7^{th} – 26^{th}) in all studied years (2001 to 2004). In general, the *Quercus robur* showed the latest UL, while the *Betula pendula* showed the earliest UL over all four years (Table 4-1).

Table 4-1. Overview of the mean (DOY) and the CV (%) for leaf unfolding and flowering dates of deciduous forest species from 2001 to 2004.

	2001		2002		2003		2004	
Leaf Unfolding	**mean**	**CV**	**mean**	**CV**	**mean**	**CV**	**mean**	**CV**
Fagus sylvatica	117.18	10.56	111.41	9.96	106.46	12.59	104.63	8.03
Quercus rubra	119.67	0.48	107.00	3.91	106.71	1.04	113.00	6.05
Quercus robur	125.15	5.22	116.07	7.90	108.19	9.56	111.15	15.50
Betula pendula	109.70	8.64	97.00	9.97	102.14	8.00	100.52	13.04
Flowering								
Crataegus monogyna	130.03	3.25	115.55	7.31	118.38	4.51	119.61	5.21
Corylus avellana	46.61	40.94	31.00	37.22	33.00	58.01	22.50	71.77
Sorbus aucuparia	130.85	3.33	119.49	4.97	118.81	3.38	122.42	3.43
Crataegus sp.	130.38	4.14	116.56	7.47	118.57	4.51	119.23	5.06
Sambucus nigra	145.50	6.42	133.56	15.16	135.47	14.08	141.90	7.32

The differences between the UL dates of the different species ranged from 6 to 19 days over the four years (19^{th} of April - 05^{th} of May 2001; 7^{th} - 26^{th} of April 2002; 12^{th} - 18^{th} of April 2003; 9^{th} – 22^{th} of April 2004). At species level, all UL dates showed a general decreasing trend, however, only the two Quercus species showed an exactly similar trend over the years. Year 2001 was characterized as the year with the latest leaf unfolding period for all species. A maximum decrease was observed from 2001 to 2002. In year 2002, leaf unfolding occurred on average 10 days earlier than the year before. From 2002 to 2004 smaller differences were observed (+- 2 days) (Figure 4-6). In year 2003 the mean leaf unfolding date reached its minimum.

Concerning the coefficient of variation (CV), no overall consistent pattern was observed. The maximum CV was observed in 2004, for all main species, with the exception of the *Fagus sylvatica* (Figure 4-6). The maximum variation in CV occurred from 2003 to 2004 for al species.

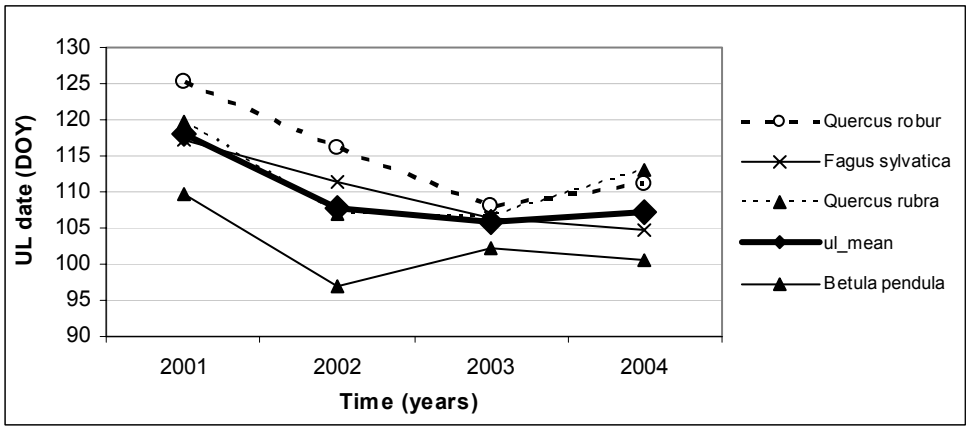

Figure 4-6. The trend of the mean UL dates of the main forest species over the years 2001 to 2004.

The blooming dates of the main understory species performed in a similar way as the UL dates. The year with the latest blooming period was also 2001, and the maximum decrease in days occurred from 2001 to 2002. In 2002, the blooming period occurred on the average 13 days earlier than in 2001 and was the earliest for most species (Figure 4-7). With regard to the CV, the flowering period performed differently. The maximum variation occurred from 2001 to 2002 for most species.

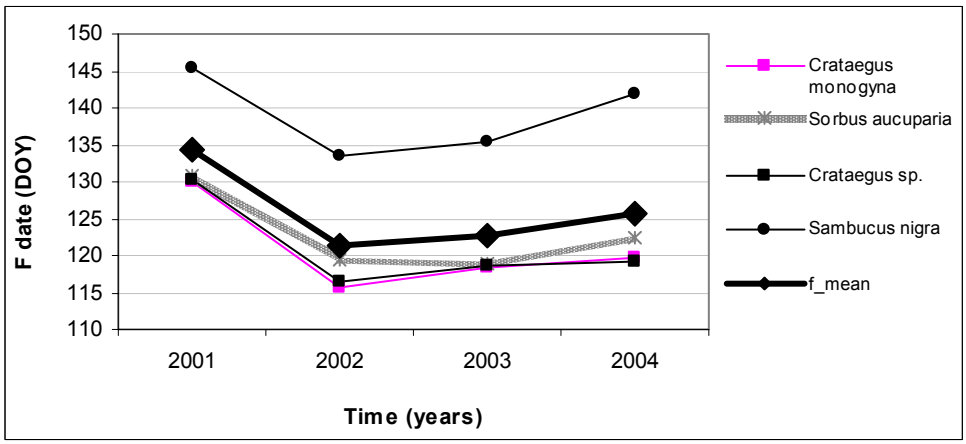

Figure 4-7. The trend of the mean F dates of the understory forest species over the years 2001 to 2004.

In general, the UL and F periods showed a decreasing trend from 2001 to 2004 for all studied species. Year 2001 was characterized as the year with the latest leaf unfolding and flowering periods. With regard to the CV, no general consistent pattern was observed for the studied species. This could indicate that the variability of the data depends on the species rather than on the environment (if we assume that environmental changes affect the species in a similar way). Or it could also be attributed to the difference in number of sample cases per observed species.

❖ Leaf fall (FL)

Field data for the phenophases Leaf Fall (FL), Colouring 50% (Cl50) and Colouring 100% (Cl100) were also analysed; however, complete timeseries were only

available for some specific species, respectively: *Quercus robur, Betula pendula and Fagus Sylvatica*. All three phenophases showed a similar decreasing trend over the studied period. Year 2001 was characterized by its late leaf fall and coloring period and was followed by a relatively large decrease of more than 10 days towards 2002 (Figure 4-8).

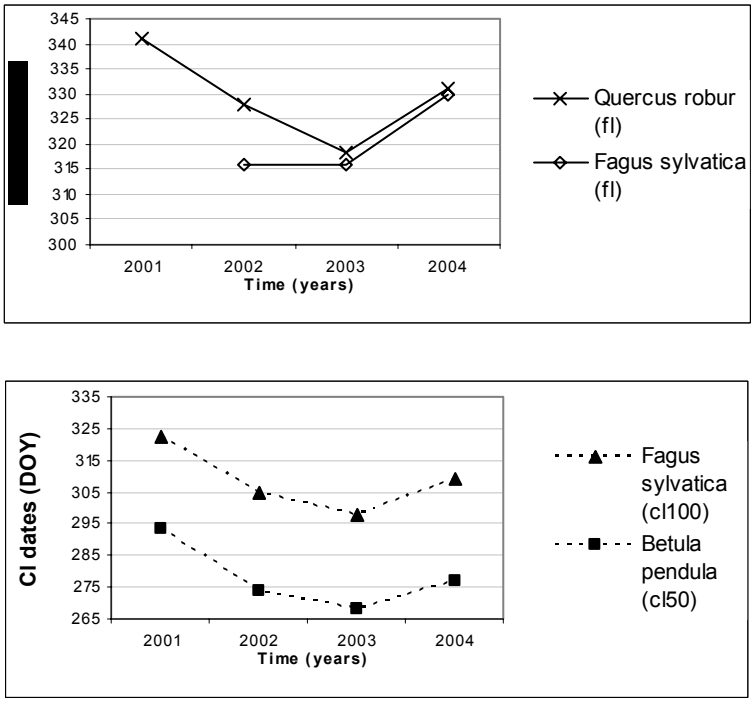

Figure 4-8. The trend of the mean FL, CL50 and Cl100 dates for the main forest species over the years 2001 to 2004

❖ Length of the growing season (GSL)

The length of the growing season (GSL) for *Fagus sylvatica* and *Quercus robur* reached a maximum mean of 222 days in year 2004. The highest deviation was from 2003 to 2004 (Figure 4-9).

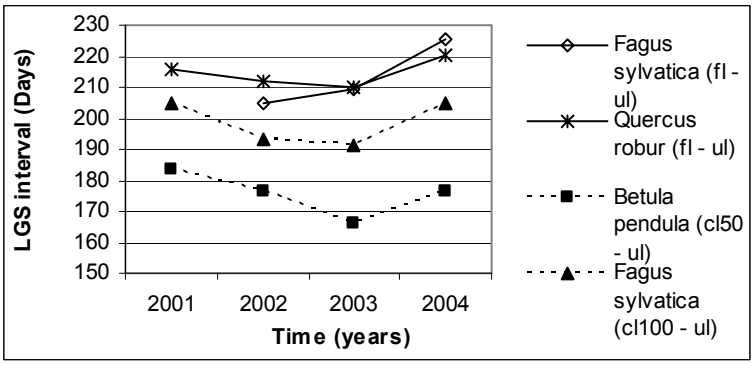

Figure 4-9. Trend of the mean Length of the growing for forest species from 2001 to 2004

4.4.2 REMOTE SENSING PHENOLOGICAL INDICATORS

❖ Start of the growing season (SOS)

From the comparison analysis of the field and RS data we observed that most SOS dates occurred from 0 to 1 16d unit later than the UL dates. Consistent differences (SOS and UL within the same 16d unit) over the four years were only observed for two methods: ***evi_hants_smns*** and ***evi_hants_deriv.*** These two methods were found to mimic the main characteristics of the UL trend of most forest species as well as the blooming trend of the understory species (Figure 4-10). At the species level, the two methods were found to mimic the UL trend of the *Fagus sylvatica* precisely within the same 16d unit over the four years (Figure 8-3).

a) Leaf unfolding and SOS dates

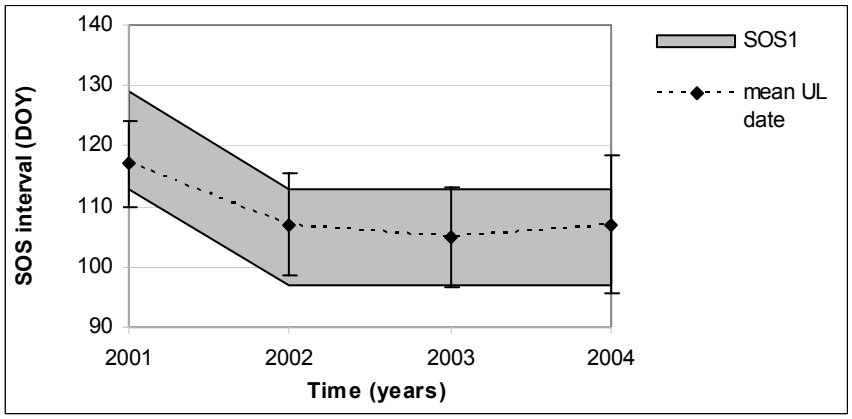

b) Blooming and SOS dates

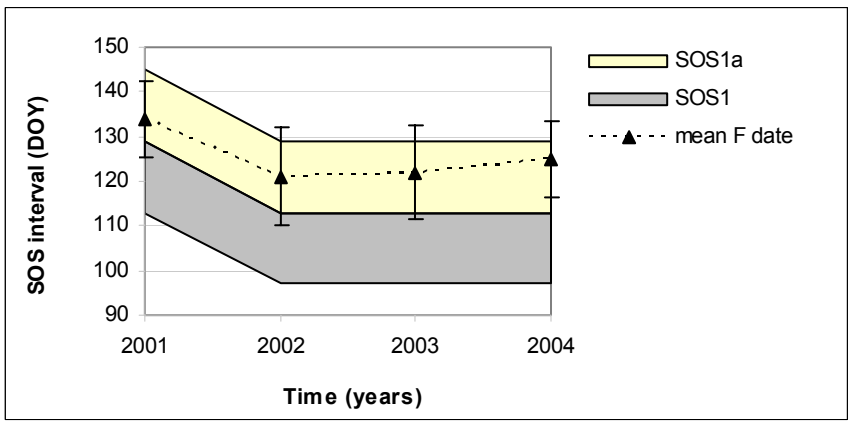

Figure 4-10. Overview of the Field and Remote sensing phenological indicators.
a) The trend of mean UL dates and SOS intervals from 2001 to 2004. SOS1 refers to the SOS interval derived by the methods ***evi_hants_smn*** and the ***evi_hants_deriv***. Mean UL refers to the mean of all species. **b)** The trend of the mean blooming dates and SOS intervals are presented for 2001 - 2004. SOS2 is the SOS interval following the SOS1 interval. SOS1 has the same meaning as explained for graph a. Mean F date refers to the mean of all species.
Error bars refer to ± one standard deviation.

❖ Variability of the SOS dates

The analysis of the variability evidenced similarity of the RS CV trends derived by the two methods (***evi_hants_smn*** and ***evi_hants_deriv)*** with the CV trend of the *Fagus sylvatica.* The CV trends of most of the other species were simulated by the ***ndvi_hants_smn*** and ***the ndvi_hants_deriv*** (Table 4-2).

Table 4-2. Similarity of RS CV trends and Field CV trends measured in sum of squares of the differences.

	ndvi_hants_smn_sos	ndvi_hants_deriv_sos
Betula pendula	111.93	260.26
Crataegus sp.	401.65	665.31
Crataegus monogyna	416.92	684.97
Sorbus aucuparia	531.50	828.77
Quercus rubra	603.68	910.97
	evi_hants_smn_sos	**evi_hants_deriv_sos**
Fagus sylvatica	65.88	112.19

❖ End of the growing season (EOS)

From the comparison of the field and RS data we observed that the EVI based EOS dates were mostly in the same range as the Cl50 field data. The NDVI based EOS dates were in the same range as the Cl100 field data. From all methods, only the ***evi_hants_deriv***. EOS dates showed similarity with the general trend of the field indicators. However, the field FL dates occurred 3 16d units later than the correspondent RS indicators (Figure 4-11).

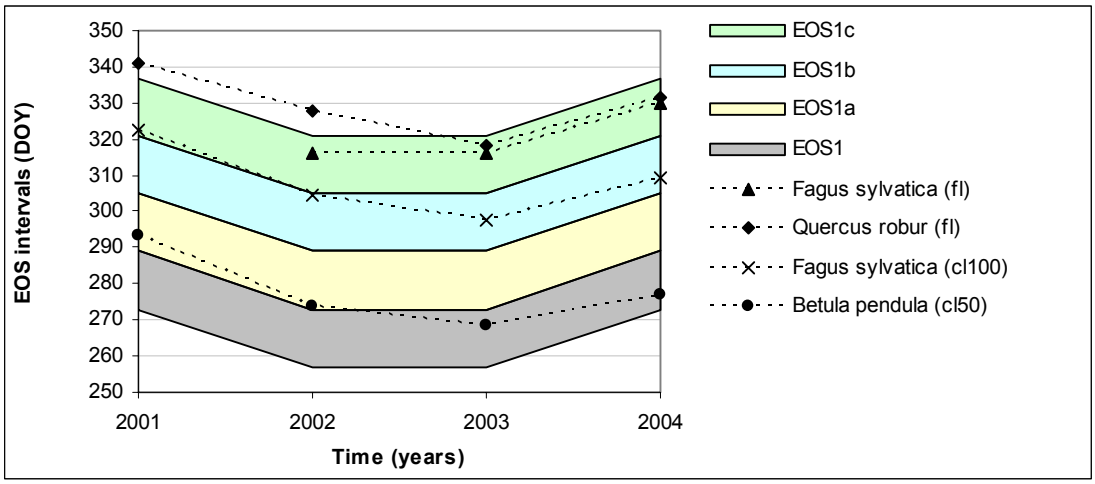

Figure 4-11. Trend of the mean EOS and FL and CL dates from 2001 – 2004.

The trend of mean FL / CL dates and EOS intervals from 2001 to 2004. EOS1 refers to the EOS interval derived by the method ***evi_hants_deriv***. EOS2 is the EOS interval following the EOS1 interval, analogously for EOS3 and EOS4.

❖ **Length of the growing season**

The analysis of the field and RS GSL intervals indicated two methods which resulted in similar GSL trends over the years: the ***evi_hants_deriv*** and the ***evi_sg_smn***. The first mentioned method seemed to follow the GSL trend of the *Fagus sylvatica* more closely, while the latter seemed to follow the GSL trend of the *Quercus robur*. RS GSL intervals were 4 16d units smaller than the field dates.

4.4.3 DISCUSSION

From all the combinations of methods, the ***evi_hants_smn*** and the ***evi_hants_deriv*** performed best in tracking the general pattern of the surface forest phenology. The SOS trend simulated the UL trend over the four years (mean UL dates were within the mean SOS interval), indicating that the corresponding indicators measure a similar greenness status (considering the temporal resolution constraint). The RS EOS was best simulated by the ***evi_hants_deriv*** but corresponded more with the colouring 50% field phase. This indication can not be generalized as the available field data for the Leaf fall were very limited, thus can not be used as representative data for this phase. With regard to the variability, only the *Fagus sylvatica* showed correspondence with the two methods. Considering the "species dependent" character of the variability as suggested by the analysis of the field data, this could indicate that the ***Fagus sylvatica*** was the dominant specie in the study area ("pure vegetation class"). On the other hand, this could also be attributed to the limited temporal resolution of the MODIS dataset. With regard to the method combination ***ndvi_hants_deriv*** and the estimation methods, the results showed consistency with the results of De Wit and Su (2004) and Schwartz et al. (2002).

4.5 ANALYSIS OF THE REMOTE SENSING INDICATORS: GRASSLAND

4.5.1 FIELD PHENOLOGICAL INDICATORS

❖ Flowering

The phenological trend of the grassland cover was quite similar to the forest cover trend (Figure 4-12). The year 2001 was characterized as the year with the latest flowering period for most of the studied species (90%). From 2001 to 2002, an overall decrease was observed, representing at the same time the highest decrease for most species. The flowering period in 2002 was on the average 10 days earlier than the year before. In 2003, most species had a relatively later flowering period (+3 days) when compared to the previous year. In 2004, flowering occurred on average 1 day earlier than in 2003. With regard to the coefficient of variation (CV), no overall consistent pattern was observed for none of the methods.

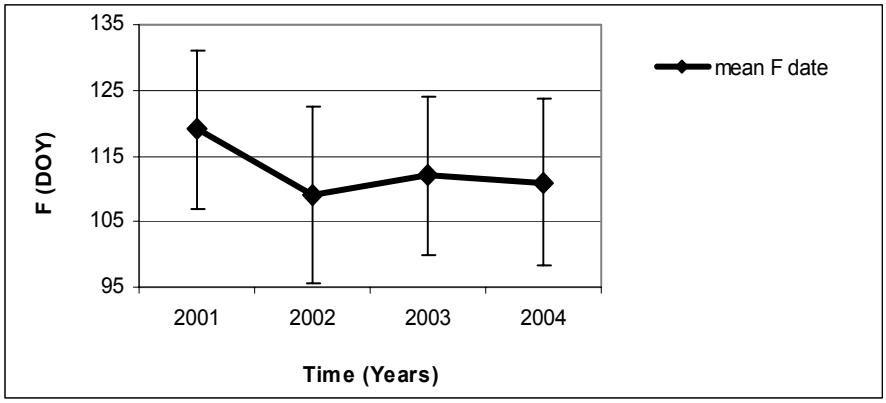

Figure 4-12. Trend of the mean F dates for grassland from 2001 – 2004.
Error bars refer to ± one standard deviation.

4.5.2 REMOTE SENSING PHENOLOGICAL INDICATORS

❖ Start of the growing season

The RS SOS dates were on average 1 16-day unit earlier than the field dates. The analysis of the results evidenced four RS methods which resulted in SOS trends similar to the flowering trend: ***ndvi_sg_deriv, ndvi_hants_deriv, evi_hants_smn and evi_hants_deriv*** (Figure 4-13). The latter two mentioned methods were found to mimic the main characteristics of most of the studied species (20 of 21), while the other two methods seem to simulate the trend of one specie, the *Daucus carota*. With regard to the variability, the methods did show consistency in the simulation of the CV trends.

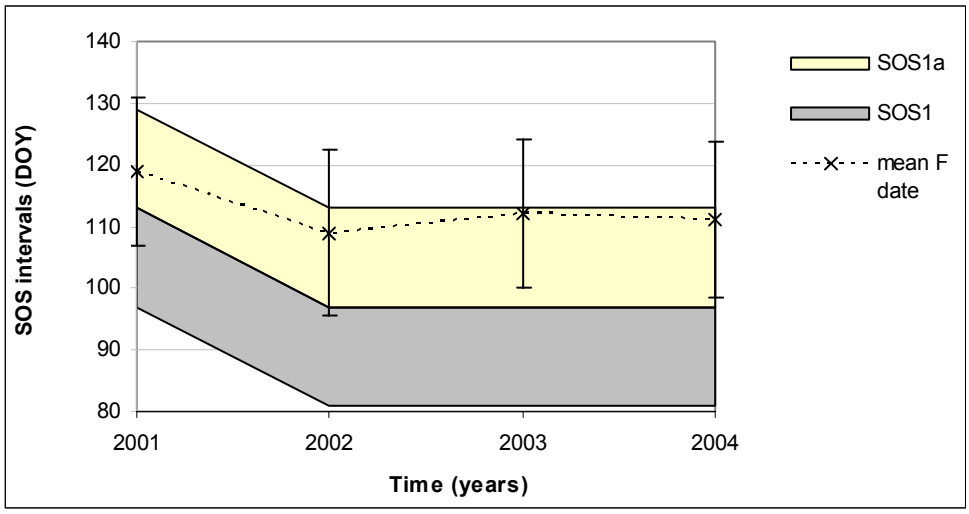

Figure 4-13. Illustration of the flowering dates and corresponding SOS dates
SOS1 refers to the SOS interval derived by the methods ***evi_hants_smn*** and ***evi_hants_deriv***. SOS2 is the SOS interval which follows the SOS1 interval.
Error bars refer to ± one standard deviation.

4.5.3 DISCUSSION

Many of the studied RS methods simulated the general flowering pattern and / or variability of the grassland cover. However, the observed methods did not show good performance in measuring both, the flowering trend and the variability, in a consistent way over the years. This could be attributed to the temporal resolution of the dataset. In addition, the grassland cover consists of a mixture of species which may not be represented by the validation species in the same composition. Among the different methods, the ***evi_hants_smn*** and the ***evi_hants_deriv*** showed superior performance in tracking the mean trend from 2001 to 2004.

4.6 ANALYSIS OF THE REMOTE SENSING INDICATORS: WINTER WHEAT

4.6.1 MODEL PHENOLOGICAL INDICATORS

The phenological indicators obtained from the WOFOST/CGMS model for winter wheat showed great similarities with the field indicators of the other classes. The year 2001 was characterized as the year with the latest SOS. From 2001 to 2002, an overall decrease was observed, representing at the same time the highest decrease for both, SOS and EOS. The SOS in 2002 was on average 20 days earlier than the year before, the EOS 10 days. The GSL reached a maximum in 2002, an average of 92 days (Figure 4-14).

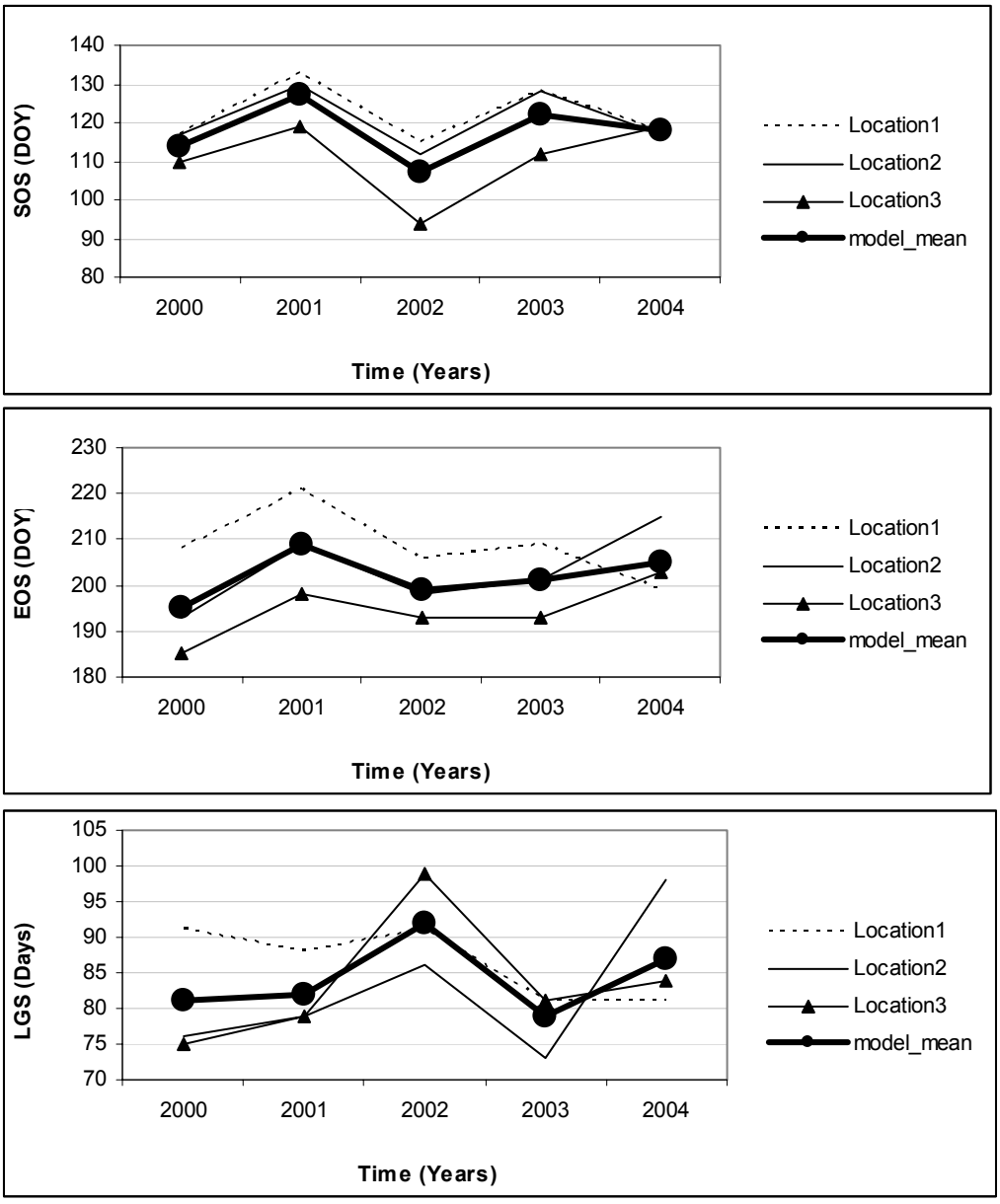

Figure 4-14. Model indicators for Winter wheat from 2000 to 2004 for the three distinct locations.

4.6.2 REMOTE SENSING PHENOLOGICAL INDICATORS

❖ **Start of the growing season**

The main trend of the model SOS was captured by the remote sensing data derived by the methods: ***ndvi_hants_smn & evi_sg_smn*** and ***evi_hants_deriv***. The general model SOS trend over the five years was not followed by any of the RSPIs (Figure 4-15).

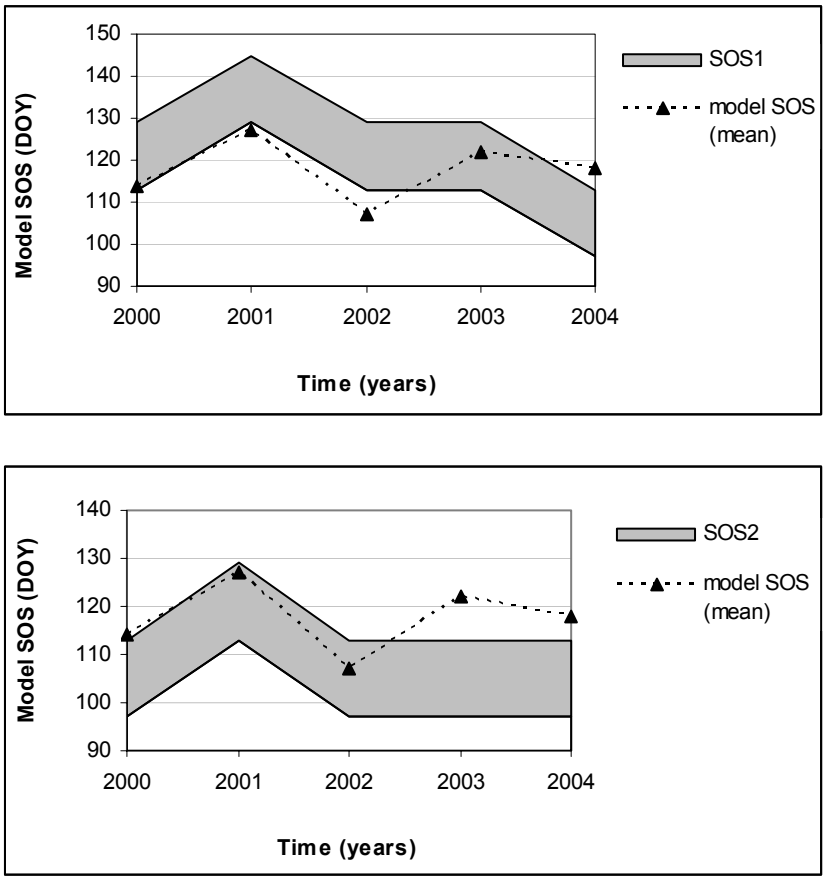

Figure 4-15. Illustration of the MODEL SOS and the corresponding Remote sensing indicators.

SOS1 refers to the SOS interval derived by the methods ***ndvi_hants_smn*** and ***evi_sg_smn***. SOS2 refers to the SOS interval derived by the ***evi_hants_deriv*** method.

❖ End of the growing season

From the three model indicators, the EOS showed the best match with its corresponding remote sensing indicators. Most of the RS methods (***ndvi_hants_smn, ndvi_hants_deriv, evi_hants_smn, evi_hants_deriv, evi_sg_smn, evi_sg_deriv)*** showed correspondence with the model EOS trend, but were between 2 and 4 16-day units later than the model EOS. The ***evi_sg_smn*** and ***evi_sg_deriv*** showed a smaller difference with the model trend. (Figure 4-16).

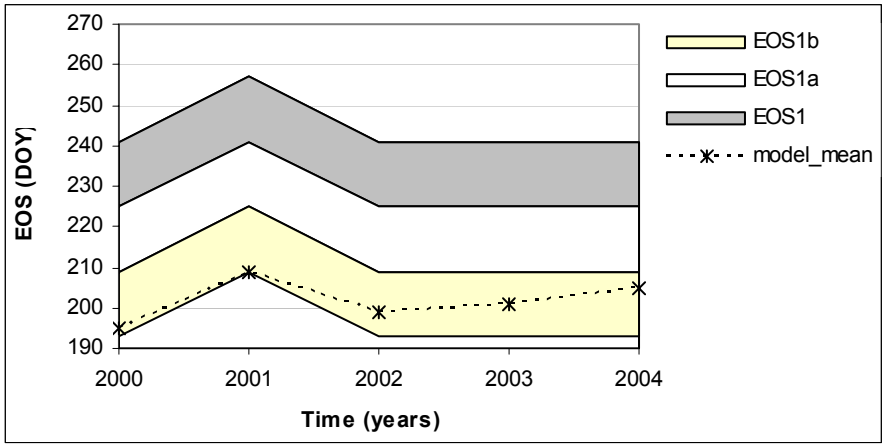

Figure 4-16. Model and RS trend of the EOS for winter wheat from 2000 to 2004

EOS1 refers to the EOS interval derived by the methods: **e*vi_sg_deriv*** and ***evi_sg_smn***. EOS1a refers to interval below the EOS1 interval. EOS1b refers to the interval which includes the EOS trend, the second interval below EOS1.

❖ Length of the growing season

None of the remote sensing methods showed success in following the GSL trend of the model indictors. The main trend characteristic, the peak in 2002 was not evidenced by the RSPIs.

4.6.3 DISCUSSION

The model indicators were derived from the modelled LAI curve. The low success of the RS indicators in simulating the MODEL SOS trend could be an indication of non consistency in the relationship between winter wheat LAI and the VIs. The maximum increase in LAI is not necessarily translated in the maximum increase in the VI time-series. On the other hand, the discrepancy could also be attributed to the MODEL itself or the temporal resolution of the MODIS data. The MODEL EOS showed better correspondence with the RS EOS. This could signal a certain correspondence between the VIs and the senescence status of the vegetation cover.

5 CONCLUSIONS

The results of this study demonstrate the applicability of the MODIS MOD13Q1 product for the monitoring of general interannual surface phenology of the forest, grassland and winter wheat covers. The relatively late UL and F period in 2001 was identified at all studied classes. The early UL and F period in 2002 was also depicted at al classes. The smaller variations were not captured by none of the methods, most likely due to the temporal resolution of the MODIS data. In general, no individual method provided consistent information about al phenophases of all vegetation classes. The results suggest that each vegetation cover and phenophase require a different combination of methods for its efficient monitoring. For monitoring of the mean UL and F dates the EVI_HANTS_DERIV method showed superior performance for all vegetation classes.

With regard to the monitoring of the different vegetation classes, the following conclusions could be drawn: (1) For the forest cover, the two EVI_HANTS combinations performed well in tracking the interannual forest phenology (SOS, EOS, GSL). The mean UL dates were simulated within the SOS interval, while the mean F dates occurred 1 16-day unit later than the mean SOS. The EOS appeared to correspond with the CL50 phase. In general, forest RSPIs showed the best performance in simulating its corresponding field indicators. (2) The grassland cover was more difficult to be related to the RS methods. Even though the general phenological trend was followed, consistency of the methods in measuring both timing and variability was rather low. Similar to the forest cover, the EVI_HANTS methods performed best in tracking the mean F trend over the four years (SOS trend was 1 16-d unit earlier than the F trend). (3) With regard to the winter wheat, the RSPIs were less successful in tracking the model trend. Only the 2001 peak and the early model SOS in 2002 were identified by the EVI_HANTS_DERIV, but a low tracking consistency was revealed for the other years. The MODEL EOS trend was simulated best by the EVI_SG methods.

In general, the analysis of the different methods revealed the differences between the two vegetation indices mainly with regard to their sensitivity to vegetation changes and the time interval. These differences seem to persist throughout the whole processing block. From the analysis of the effect of the different methods on the RSPIs we concluded the following: (1) The EVI based RSPIs appeared to be more sensitive for variances in the vegetation status and seem to overcome the time unit constraint for detection of the interannual phenology trend. (2) The combination of the EVI with the HANTS smoothing method and any of the estimation method seems to be a promising method for the estimation of RSPIs of all classes. (3) The SG based methods performed well in reconstructing the VI time series. The parameters are simple to be set, however, the estimation methods were not very suitable for the derivation of the RSPIs. This smoothing method has its potential in providing more accurate information on phenological metrics as: maximum NDVI and multi modality. (4) With regard to the estimation methods, it appears that the vegetation status identified by them depends on the vegetation class and the processing steps.

The analysis of the effect of the pixel purity on the RSPIs showed us that when using the MOD13Q1 product for phenological monitoring purposes of the three

classes in the Netherlands, it is mostly important to work with “pure pixels”. The use of the complete vegetation cover will affect the accuracy of the indicators, considering the poor correspondence observed between the “pure” pixel vegetation classes and the “al pixel” vegetation classes.

The most general conclusion to be drawn from this study is that RSPIs highly depend on the relationship between the Vegetation class, the VIs and all subsequent processing steps. It seems to be most fundamental to understand the measuring extent of the VIs since these characteristics seem to persist throughout the whole process. The relationship between the methods and the vegetation covers need to be studied more deeply, and longer time series are needed to draw better conclusions.

6 RECOMMENDATIONS

The results of this study were found promising. To improve studies within this context, it is important to consider the weakness of this study:

- Spatial resolution of the dataset: the spatial resolution of 250 m provides more accurate information than the 500 and 1-km datasets. However, the image resolution and the pixel-based approach result in huge amounts of data to be processed. It is therefore important to focus on the development of an automated process. High importance should also be given to the pixel purity. One should work as much as possible with "pure" pixels to guarantee higher accuracy of the indicators.

- Temporal resolution: for general interannual phenology the temporal resolution seems satisfactory. For a more detailed analysis, efforts should be made to scale down this resolution: this can be by smaller composite VI data or by interpolation methods. With regard to interpolation methods it would be more accurate to apply them to smoothed daily VI time –series. By doing so, we can guarantee the real positions of peaks, especially when using the SG method for smoothing.

- Studies on the VIs, the smoothing methods, the estimation methods, the indicators, the vegetation covers and their interrelationships should be accomplished to increase the understanding of the relevant relationships:

    - Biophysical vegetation variables (LAI / fCOV / fPAR) – Field phenophases (mainly leaf production, stability, senescence) (correlation / regression studies for the purpose of defining which phenophase is best explained by which biophysical variable);

    - Biophysical vegetation variables (LAI / fCOV / fPAR) - VI (correlation / regression studies for the purpose of defining which VI is best related to which biophysical variable. Studies on the application of spectral mixing analysis can also be explored;

    - VI – Field phenophase (correlation / regression studies for the purpose of development of estimation methods);

    - RSPI – Field phenophases (correlation / regression studies for prediction purposes)

  Finally, it would be important to combine existing datasets from different sources, such as: the forest inventory dataset, the Natuurkalender data, Remote sensing data, results of remote sensing studies within the Netherlands. The possibilities of the development of a phenology map based on these data should be studied as well.

7 REFERENCES

Badhwar, G. D. (1984). Use of Landsat-derived profile features for spring small-grains classification, *Int. J. Remote Sensing*, 5(5), 783-797.

Blanch Roure, S. J. (2003). Analysis of the phenological changes of the vegetation in the netherlands by using a multitemporal treatment of satellite images, *MSC Thesis,* 89 pages.

Botta A., Viovy N., Ciais P., Friedlingstein P., Monfray P. (2000). A global prognostic scheme of leaf onset using satellite data. *Global Change Biology*, 6(7), 709-725.

Chen, J., Jonsson, P., Tamura, M., Gu, Z., Matsushita, B., Eklundh, L. (2004). A simple method for reconstructing a high-quality NDVI time-series data set based on the Savitzky–Golay filter. *Remote Sensing of Environment*, 91, 332–344.

Chen, X., Tan, Z., Schwartz, M. D., Xu, C. (2000). Determining the growing season of land vegetation on the basis of plant phenology and satellite data in Northern China. *Int. J. Biometeorol*, 44, 97 – 101.

Chuine, I. (2000). A unified model for budburst of trees. *J. Theor. Biol.*, 207, 337–347.

Clevers, J. Bartholomeus, H.; Mücher, C., De Wit, A. (2004). Use Of Meris Data For Land Cover Mapping In The Netherlands. *Proc. MERIS User Workshop*, Frascati, Italy, 10 – 13 November 2003. (ESA SP-549, May 2004).

De Wit, A. (2004). The IDL-ENVI implementation of the HANTS algorithm. *WUR – CGI, Wageningen.*

De Wit, A.J.W. Su, B. (2004). Deriving phenological indicators from SPOT-VGT data using the HANTS Algorithm. *Centre for Geo-information*.

Duchemin B., Goubier J., Courrier G. (1999). Monitoring phenological key stages and cycle duration of temperate deciduous forest ecosystems with NOAA/AVHRR data, *Remote Sensing of Environment*, 67(1), 68-82.

EPN (2004). Http://www.dow.wau.nl/msa/gpm, 21/06/2004

EOS-MODIS. (2004). http:// edcimswww.cr.usgs.gov/ pub/ imswelcome, 22/12/204

EOS-TBRS. (2004). http://tbrs.arizona.edu/project/MODIS/index.php, 22/12/2004

Ferreira L.G., Huete A.R. (2004). Assessing the seasonal dynamics of the Brazilian Cerrado vegetation through the use of spectral vegetation indices, *International Journal of Remote Sensing*, 25(10), 1837-1860.

Huete, A. R., Liu,H. Q., Batchily, K., Leeuwen, W. van. (1997). A Comparison of Vegetation Indices over a Global Set of TM Images for EOS-MODIS. *Remote sensing of environment*, 59(3), 440-451.

Huete A., Didan K., Miura T., Rodriguez E.P., Gao X., Ferreira L.G. (2002). Overview of the radiometric and biophysical performance of the MODIS vegetation indices. *Remote Sensing of Environment*, 83(1-2), 195-213.

Justice C.O., Townshend J.R.G., Holben B.N., Tucker C.J. (1984) Analysis of the phenology of global vegetation using meteorological satellite data. *International Journal of Remote Sensing*, 6(8), 1271-1318.

Justice C.O., Holben B.N., Gwynne M.D. (1986). Monitoring East African vegetation using AVHRR data., *International Journal of Remote Sensing*, 7(11), 1453-1474.

Justice C.O., Townshend J.R.G., Choudhury B.J. (1989). Comparison of AVHRR and SMMR data for monitoring vegetation phenology on a continental scale, *International Journal of Remote Sensing*, 10(10), 1607-1632.

Kaduk, J., Heimann, M. (1996). A prognostic phenology scheme for global terrestrial carbon cycle models, *Clim. Res., 6*, 1-19.

Kasischke E.S., French N.H.F. (1997). Constraints on using AVHRR composite index imagery to study patterns of vegetation cover in boreal forests, *International Journal of Remote Sensing*, 18(11), 2403-2426.

Mauser W. (1986). Multi-temporal analysis of the phenological stage of vegetation using tm-data in the southern black forest. *Digest - International Geoscience and Remote Sensing Symposium* (IGARSS), 1461-1464.

Menzel, A. (2000). Trends in phenolgogical phases in Europe between 1951 and 1996. *Int J Biometeorol*, 44, 76–81.

Moulin S., Kergoat L., Viovy N., Dedieu G. (1997). Global-scale assessment of vegetation phenology using NOAA/AVHRR satellite measurements, *Journal of Climate*, 10(6), 1154-1170.

Nagler, P. L. Glenn, E. P., Huete, A. R. (2001). Assesment of spectral vegetation indices for riparian vegetation in the Colorado River delta, Mexico, *Journal of Arid Environments*, 49(1), 91 – 110.

Pax-Lenney, M. Woodcock, C. (1997). The Effect of Spatial Resolution on the Ability to Monitor the Status of Agricultural Lands. *Remote sens. Environment.* 61, 210-220.

Peddle. D.R., Brunke, S. P. Hall, F.G. (2001). A comparison of spectral mixture analysis and ten vegetation indices for estimating Boreal forest biophysical information from airborne data. *Canadian Jornal of Remote Sensing*, 27(6), 627 – 635.

Privette J.L., Myneni R.B., Knyazikhin Y., Mukelabai M., Roberts G., Tian Y., Wang Y., Leblanc S.G. (2002). Early spatial and temporal validation of MODIS LAI product in the southern Africa Kalahari, *Remote Sensing of Environment*, 83(1-2), 232-243.

Reed B.C., Brown J.F., Vanderzee D., Loveland T.R., Merchant J.W., Ohlen D.O. (1994). Measuring phenological variability from satellite imagery, *Journal of Vegetation Science*, 5(5), 703-714.

Ricotta C., Avena G.C. (2000). The remote sensing approach in broad-scale phenological studies, *Applied Vegetation Science,* 3(1), 117-122.

Roerink, G. J., Menenti, M., Verhoef, W. (2000). Reconstructing cloudfree NDVI composites using Fourier analysis of time series. *Int. J. of Rem. Sens.* 21(9), 1911-1917.

Schwartz M. D. (1999). Advancing to full bloom: planning phenological research for the 21st century. *Int. J. Biometeorol.* 42, 114-118.

Schwartz, M. D., Reed, B. C. (1999). Surface phenology and satellite sensor-derived onset of greenness: an initial comparison. *Int. J. Remote sensing*, 20(17), 3451 – 3457.

Schwartz M.D., Reed B.C., White M.A. (2002). Assesing satellite-derived start-of-season measures in the conterminous USA. *International Journal of Climatology*, 22(14), 1793-1805.

Schwartz M. D. (2003). Phenology: An integrative Environmental Science. Kluwer Academic Publishers, Boston, Dordrecht, London, 564 pages.

Teillet, P.; Staenx, K.; Williams, D. (1997). Effects of Spectral, Spatial, and Radiometric Characteristics on Remote Sensing Vegetation Indices of Forested Regions. *Remote sens. Environ.* 61:139-149.

Townshend J.R.G., Justice C.O. (1986). Analysis of the dynamics of African vegetation using the normalized difference vegetation index., *International Journal of Remote Sensing*, 7(11), 1435-1445.

Van Vliet A.J.H., De Groot R.S., Clevers J., Estreguil C., Maggi M., Menzel A., Bellens Y., Braun P., Bruegger R., Bruns E., Flechsig M., Jeanneret F., Martens P., Menne B., Sparks T. (2003). The European Phenology Network. *International Journal of Biometeorology*, 47(4), 202-212.

White, M.A., Nemani, R.R., Thornton, P.E., Running, S.W. (2002). Satellite evidence of phenological differences between urbanized and rural areas of the eastern United States decicuous broadleaf forest. *Ecosystems* 5: 260 – 273.

Zhang X., Friedl M.A., Schaaf C.B., Strahler A.H., Hodges J.C.F., Gao F. (2002). Using MODIS data to study the relation between climatic spatial variability and vegetation phenology in northern high latitudes, *International Geoscience and Remote Sensing Symposium* (IGARSS), 2, 1149-1151.

Xiao, X., Braswell, B., Zhang, Q., Boles, S., Frolking, S., Moore III, B. (2002). Sensitivity of vegetation indices to atmospheric aerosols: continental-scale observations in Northern Asia. *Remote Sensing of Environment*, 84, 385 – 392.

Xin, J., Yu, Z., Leeuwen, L. van, Driessen, P. M. (2002). Mapping crop key phenological stages in the North China plain using NOAA time series images. *Int. J. Applied Earth Observation and Geoinformation,* 4, 109 – 117.

Zhang X., Friedl M.A., Schaaf C.B., Strahler A.H., Hodges J.C.F., Gao F., Reed B.C., Huete A. (2003). Monitoring vegetation phenology using MODIS, Remote Sensing of Environment, 84(3), 471-475.

Websites

MODIS data

1. http://edcimswww.cr.usgs.gov/pub/imswelcome/
2. http://modis.gsfc.nasa.gov/
4. http://edcdaac.usgs.gov/datapool/datapool.asp
5. http://tbrs.arizona.edu/project/MODIS/UserGuide_doc.php#Fileformat1

Landcover data

1. http://www.alterra.wur.nl/NL/cgi/LGN/LGN4/

Validation data

1. http://natuurkalender.nl/
2. http://www.supit.cistron.nl/start.htm

8 APPENDIX

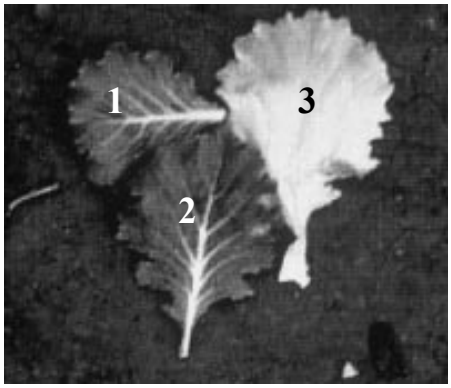

Digital photo taken with a red filter, so only red light was detected. The two green leaves are very dark, as most of the red light is absorbed by chlorophyll. The yellow leaf appears much brighter since there is no chlorophyll to absorb red light. Also note the white and black stones in the lower right of each image.

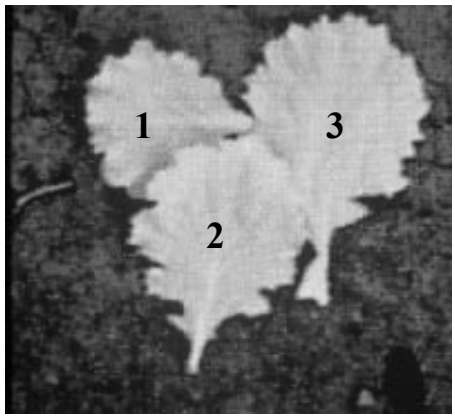

Digital photo taken with a near infrared red filter, so only near infrared light was detected. All three leaves are bright at this wavelength.due to the high reflectance caused by the leaf structure (mesophyll region). Also note the white and black stones in the lower right of each image.

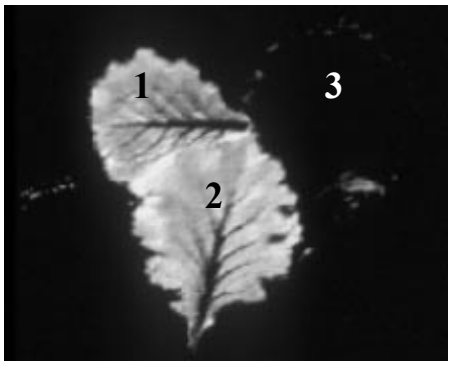

This image is the result of subtracting the red image from the near-infrared image in combination with some mathematical processing (Soil Adjusted Vegetation Index SAVI). Notice that even the ribs of the green leaves disappear since there is no chlorophyll in that part of the leaf. The little patch of green on the mostly yellow leaf is about the only part of that leaf still visible. The soil and stones have completely disappeared.

Figure 8-1. Overview of the general performance of Vegetation Indices adapted from US Water Conservation Laboratory, 2005
Three leaves were placed on a bare soil. Leave 1 and 2 were healthy green leaves. Leave 3 was yellow with a spot of pale green.
Adapted from: US Water Conservation Laboratory (2005).
http://www.uswcl.ars.ag.gov/epd/remsen/vi/VIWorks.htm

Table 8-1. Phenological data for main forest species for 2001 and 2002 (Natuurkalender)

Main Forest																
			2001							**2002**						
Scientific name	**English name**	**Soort**	**gemid.**	**med.**	**min**	**max**	**N**	**Stdev**	**Datum**	**gemid.**	**med.**	**min**	**max**	**N**	**Stdev**	**Datum**
Fagus sylvatica	*Beech*	Beuk, bladontplooiing	117.18	119.00	83	137	40	12.37	27-apr-01	111.41	111.00	78	132	29	11.10	21-apr-02
Quercus rubra	*Red Oak*	eik, Amerikaanse-, bladontplooing	119.67	120.00	119	120	3	0.58	29-apr-01	107.00	108.00	101	112	5	4.18	17-apr-02
Quercus robur	*Pedunculate oak*	eik, Zomer-, bladontplooiing	125.15	125.00	117	138	13	6.53	5-mei-01	116.07	113.00	102	135	15	9.17	26-apr-02
Betula pendula	*Silver birch*	Ruwe berk, bladontplooiing	109.70	113.00	96	123	23	9.48	19-apr-01	97.00	93.00	82	120	27	9.67	7-apr-02
Betula pendula	*Silver birch*	Berk, bloei	112.77	112.00	83	132	13	13.72	22-apr-01	88.29	93.00	33	115	24	21.76	29-mrt-02
Quercus rubra	*Red Oak*	eik, Amerikaanse-, vruchten rijp														
Fagus sylvatica	*Beech*	Beuk, herfsttint 50%								283.33	285.00	273	292	3	9.61	10-okt-02
Quercus rubra	*Red Oak*	eik, Amerikaanse-, herfsttint 50%								285.00	285.00	284	286	2	1.41	12-okt-02
Quercus robur	*Pedunculate oak*	eik, Zomer-, herfsttint 50%								290.75	294.50	274	300	4	11.81	17-okt-02
Betula pendula	*Silver birch*	Berk, Herfsttint 50%	293.25	298.00	264	313	4	20.74	20-okt-01	273.71	283.00	214	295	7	27.83	30-sep-02
Fagus sylvatica	*Beech*	Beuk, volledige herfsttint	322.33	322.50	313	330	6	6.98	18-nov-01	304.67	306.50	294	311	6	7.00	31-okt-02
Quercus rubra	*Red Oak*	eik, Amerikaanse-, herfsttint 100%														
Fagus sylvatica	*Beech*	Beuk, einde bladval								316.00	316.00	302	330	3	14.00	12-nov-02
Quercus rubra	*Red Oak*	eik, Amerikaanse-, einde bladval														
Quercus robur	*Pedunculate oak*	eik, Zomer-, einde bladval	341.00	342.00	336	345	3	4.58	7-dec-01	327.71	328.00	316	336	7	7.13	23-nov-02
Betula pendula	*Silver birch*	Berk, einde bladval	329.50	329.50	323	336	4	5.69	25-nov-01	300.90	309.00	208	336	10	33.94	27-okt-02

Table 8-2. Phenological data for main forest species for 2003 and 2004 (Natuurkalender)

Main Forest																
			2003							2004						
Scientific name	**English name**	**Soort**	**gemid.**	**med.**	**min**	**max**	**N**	**Stdev**	**Datum**	**gemid.**	**med.**	**min**	**max**	**N**	**Stdev**	**Datum**
Fagus sylvatica	*Beech*	Beuk, bladontplooiing	106.46	109.00	57	119	39	13.40	16-apr-03	104.63	106.00	76	128	67	8.40	13-apr-04
Quercus rubra	*Red Oak*	eik, Amerikaanse-, bladontplooing	106.71	107.00	105	108	7	1.11	16-apr-03	113.00	112.00	99	128	15	6.83	22-apr-04
Quercus robur	*Pedunculate oak*	eik, Zomer-, bladontplooiing	108.19	109.50	65	124	32	10.34	18-apr-03	111.15	114.00	7	123	41	17.23	20-apr-04
Betula pendula	*Silver birch*	Ruwe berk, bladontplooiing	102.14	103.00	89	115	14	8.17	12-apr-03	100.52	96.50	88	155	50	13.11	9-apr-04
Betula pendula	*Silver birch*	Berk, bloei	105.45	107.00	85	118	11	9.93	15-apr-03	98.44	99.00	46	117	27	12.73	7-apr-04
Quercus rubra	*Red Oak*	eik, Amerikaanse-, vruchten rijp	225.50	225.50	213	238	2	17.68	13-aug-03							
Fagus sylvatica	*Beech*	Beuk, herfsttint 50%	270.33	288.00	234	289	3	31.47	27-sep-03	285.63	291.00	249	304	8	18.07	11-okt-04
Quercus rubra	*Red Oak*	eik, Amerikaanse-, herfsttint 50%	285.67	293.50	264	294	6	13.00	12-okt-03							
Quercus robur	*Pedunculate oak*	eik, Zomer-, herfsttint 50%	262.50	262.50	234	291	2	40.31	19-sep-03							
Betula pendula	*Silver birch*	Berk, Herfsttint 50%	268.42	281.50	170	299	12	38.78	25-sep-03	277.20	279.00	233	307	10	23.25	3-okt-04
Fagus sylvatica	*Beech*	Beuk, volledige herfsttint	297.67	297.00	290	306	3	8.02	24-okt-03	309.40	311.00	305	312	5	2.88	4-nov-04
Quercus rubra	*Red Oak*	eik, Amerikaanse-, herfsttint 100%	302.63	305.00	294	307	8	5.07	29-okt-03							
Fagus sylvatica	*Beech*	Beuk, einde bladval	316.00	316.00	314	318	2	2.83	12-nov-03	330.00	330.00	326	334	3	4.00	25-nov-04
Quercus rubra	*Red Oak*	eik, Amerikaanse-, einde bladval	317.25	318.50	307	325	4	9.18	13-nov-03	315.00	312.00	305	326	7	7.23	10-nov-04
Quercus robur	*Pedunculate oak*	eik, Zomer-, einde bladval	318.50	318.50	318	319	2	0.71	14-nov-03	331.22	331.00	324	342	9	5.45	26-nov-04
Betula pendula	*Silver birch*	Berk, einde bladval								308.20	307.50	279	337	10	16.95	3-nov-04

Table 8-3. Phenological data for understory forest species for 2001 and 2002 (Natuurkalender)

Understory Forest																
			2001							2002						
Scientific name	**English name**	**Soort**	**gemid.**	**med.**	**min**	**max**	**N**	**Stdev**	**Datum**	**gemid.**	**med.**	**min**	**max**	**N**	**Stdev**	**Datum**
Crataegus monogyna	*Hawthorn*	Eenstijlige Meidoorn, bloei	130.03	131.00	117	138	29	4.22	10-mei-01	115.55	116.50	97	131	38	8.44	25-apr-02
Corylus avellana	*Hazel*	Hazelaar, bloei	46.61	41.00	1	80	36	19.08	15-feb-01	31.00	31.00	6	60	40	11.54	30-jan-02
Sorbus aucuparia	*Rowan, Quicken tree*	Lijsterbes, bloei	130.85	132.00	113	136	33	4.36	10-mei-01	119.49	120.00	105	130	51	5.93	29-apr-02
Crataegus sp.	*Crataegus sp.*	Meidoorn (1 en 2-stijlig), bloei	130.38	132.00	113	143	39	5.40	10-mei-01	116.56	116.00	97	135	59	8.71	26-apr-02
Sambucus nigra	*Elder*	Vlier, bloei	145.50	146.00	123	168	38	9.34	25-mei-01	133.56	136.00	51	173	55	20.24	13-mei-02
Corylus avellana	*Hazel*	Hazelaar, vruchten rijp	252.50	249.50	227	275	6	17.57	9-sep-01	248.40	248.50	201	284	10	21.28	5-sep-02
Sorbus aucuparia	*Rowan, Quicken tree*	Lijsterbes, vruchten rijp	205.11	200.00	191	227	19	11.99	24-jul-01	202.41	196.00	170	239	17	17.79	21-jul-02
Sambucus nigra	*Elder*	Vlier, vruchten rijp	226.25	227.00	212	238	12	8.21	14-aug-01	220.60	224.50	201	235	10	11.77	8-aug-02

Table 8-4. Phenological data for understory forest species for 2003 and 2004 (Natuurkalender)

Understory Forest																
			2003							2004						
Scientific name	**English name**	**Soort**	**gemid.**	**med.**	**min**	**max**	**N**	**Stdev**	**Datum**	**gemid.**	**med.**	**min**	**max**	**N**	**Stdev**	**Datum**
Crataegus monogyna	*Hawthorn*	Eenstijlige Meidoorn, bloei	118.38	118.50	102	130	40	5.34	28-apr-03	119.61	121.00	95	131	57	6.24	28-apr-04
Corylus avellana	*Hazel*	Hazelaar, bloei	33.00	33.00	3	78	75	19.14	6-feb-03	22.50	22.50	1	60	56	16.15	23-jan-04
Sorbus aucuparia	*Rowan, Quicken tree*	Lijsterbes, bloei	118.81	119.00	111	126	37	4.01	28-apr-03	122.42	122.00	109	135	50	4.20	1-mei-04
Crataegus sp.	*Crataegus sp.*	Meidoorn (1 en 2-stijlig), bloei	118.57	119.00	102	133	60	5.35	28-apr-03	119.23	119.00	95	131	71	6.04	28-apr-04
Sambucus nigra	*Elder*	Vlier, bloei	135.47	138.00	40	177	51	19.07	15-mei-03	141.90	142.00	116	166	49	10.38	20-mei-04
Corylus avellana	*Hazel*	Hazelaar, vruchten rijp	218.25	210.00	193	265	8	24.81	6-aug-03	230.28	226.50	183	264	18	18.58	17-aug-04
Sorbus aucuparia	*Rowan, Quicken tree*	Lijsterbes, vruchten rijp	197.36	193.00	177	231	28	13.98	16-jul-03	209.95	201.00	194	240	21	15.25	27-jul-04
Sambucus nigra	*Elder*	Vlier, vruchten rijp	218.45	220.50	199	229	22	9.43	6-aug-03							

Table 8-5. Phenological data for grassland species for 2001 and 2002 (Natuurkalender)

Grassland species																
			2001							2002						
Scientific name	English name	Soort	gemid.	med.	min	max	N	Stdev	Datum	gemid.	med.	min	max	N	Stdev	Datum
Cerastium arvense	*Mouse-ear chickweed*	Akkerhoornbloem	119.83	120.00	83	141	35	13.48	29-apr-01	107.44	110.00	51	131	39	15.25	17-apr-02
Tanacetum vulgare	*Tansy*	Boerenwormkruid	188.28	190.00	165	216	25	12.57	7-jul-01	188.00	188.00	170	204	19	10.06	7-jul-02
Cytisus scoparius	*Broom*	Brem, bloei	116.20	118.00	82	133	49	11.55	26-apr-01	99.05	103.50	32	126	64	18.65	9-apr-02
Caltha palustris	*King-cub, Marsh marigold*	Dotterbloem	92.51	93.00	43	118	81	13.82	2-apr-01	83.23	83.00	43	110	107	12.28	24-mrt-02
Anthriscus sylvestris	*Cow-parsley*	Fluitekruid	112.40	117.50	45	144	106	16.26	22-apr-01	96.61	98.00	32	130	109	17.82	6-apr-02
Holcus lanatus	*Yorkshire-fog*	Gestreepte witbol														
Laburnum anagyroides	*Laburnum*	Gouden regen, bloei	135.14	135.00	126	146	35	4.90	15-mei-01	123.00	123.00	78	147	43	11.27	2-mei-02
Malva sylvestris	*Common Mallow*	Groot kaasjeskruid								176.96	177.00	140	215	24	16.94	25-jun-02
Lythrum salicaria	*Purple Loosestrife*	Grote kattenstaart	188.20	188.00	181	199	5	6.83	7-jul-01	177.94	178.50	161	187	16	7.74	26-jun-02
Alopecurus pratensis	*Meadow Foxtail*	Grote vossenstaart														
Glechoma hederacea	*Ground ivy*	Hondsdraf	97.88	98.50	38	118	66	13.10	7-apr-01	85.53	86.00	41	112	104	13.68	26-mrt-02
Tussilago farfara	*Colt's foot*	Klein hoefblad	65.55	69.00	37	95	94	15.63	6-mrt-01	55.56	55.00	25	92	124	13.89	24-feb-02
Lychnis flos-cuculi	*Ragged robin*	Koekoeksbloem, Echte, bloei	131.26	131.00	111	156	65	8.02	11-mei-01	124.14	125.50	91	154	72	11.59	4-mei-02
Dactylis glomerata	*Cock's-foot*	Kropaar														
Ranunculus repens	*Creeping buttercup*	Kruipende boterbloem	122.22	127.00	43	134	32	16.69	2-mei-01	115.32	118.00	33	143	41	19.54	25-apr-02
Alliaria petiolata	*Garlic mustard*	Look zonder look	121.03	121.50	94	136	64	7.22	1-mei-01	108.36	109.00	69	132	81	9.00	18-apr-02
Viola odorata	*Sweet violet*	Maarts viooltje	81.05	81.00	52	106	66	12.29	22-mrt-01	61.10	61.00	10	105	89	17.35	2-mrt-02
Leucanthemum vulgaris	*Ox-eye daisy*	Margriet, Gewone, bloei	140.71	138.50	128	153	28	6.98	20-mei-01	132.25	132.00	96	150	55	9.98	12-mei-02
Stachys palustris	*Marsh Woundwort*	Moerasandoorn								181.33	177.00	163	217	6	18.66	30-jun-02
Filipendula ulmaria	*Meadow-sweet*	Moerasspirea	184.09	185.00	167	199	11	10.94	3-jul-01	176.93	176.00	159	201	15	11.56	25-jun-02
Cardamine pratensis	*Cuckoo-flower, Lady's smock*	Pinksterbloem	104.12	103.00	62	134	139	10.97	14-apr-01	89.64	89.00	66	119	135	8.90	30-mrt-02
Ranunculus acris	*Meadow buttercup*	Scherpe boterbloem	120.82	124.50	88	137	44	11.76	30-apr-01	105.32	106.00	40	130	62	15.25	15-apr-02
Galanthus nivalis	*Snow drop*	Sneeuwklokje	29.35	36.00	-46	69	105	18.38	29-jan-01	28.45	32.00	-42	59	113	15.31	28-jan-02
Ranunculus ficaria	*Small selandine*	Speenkruid	66.45	68.50	-20	101	156	19.65	7-mrt-01	60.69	63.00	-24	97	166	15.15	1-mrt-02
Hypericum perforatum	*common St. Johnswort*	St. janskruid	177.67	177.00	158	190	15	9.31	26-jun-01	172.50	172.50	135	204	18	15.98	21-jun-02
Phleum pratense	*Timothy*	Timoteegras														
Daucus carota	*Wild Carrot*	Wilde peen	189.83	190.00	182	197	6	7.17	8-jul-01	190.73	193.00	159	205	11	12.95	9-jul-02
Lamium album	*White deadnettle*	Witte dovenetel	111.59	114.00	77	146	66	14.15	21-apr-01	94.28	93.00	34	134	92	13.79	4-apr-02

Table 8-6. Phenological data for grassland species for 2003 and 2004 (Natuurkalender)

Grassland species																
			2003							2004						
Scientific name	English name	Soort	gemid.	med.	min	max	N	Stdev	Datum	gemid.	med.	min	max	N	Stdev	Datum
Cerastium arvense	*Mouse-ear chickweed*	Akkerhoornbloem	111.81	111.00	90	138	47	10.77	21-apr-03	105.06	107.00	67	128	35	11.62	14-apr-04
Tanacetum vulgare	*Tansy*	Boerenwormkruid	180.32	182.00	146	224	37	16.12	29-jun-03	183.17	184.50	154	198	18	12.75	1-jul-04
Cytisus scoparius	*Broom*	Brem, bloei	109.87	111.00	39	125	47	13.31	19-apr-03	108.90	114.00	43	124	51	16.99	17-apr-04
Caltha palustris	*King-cub, Marsh marigold*	Dotterbloem	92.21	91.00	68	115	107	10.14	2-apr-03	87.11	90.00	5	120	107	18.44	27-mrt-04
Anthriscus sylvestris	*Cow-parsley*	Fluitekruid	108.21	109.00	86	131	123	8.14	18-apr-03	100.66	103.00	34	122	158	14.31	9-apr-04
Holcus lanatus	*Yorkshire-fog*	Gestreepte witbol								142.64	141.00	131	165	11	9.72	21-mei-04
Laburnum anagyroides	*Laburnum*	Gouden regen, bloei	122.50	122.50	102	137	36	6.70	2-mei-03	124.00	124.00	114	137	36	5.01	2-mei-04
Malva sylvestris	*Common Mallow*	Groot kaasjeskruid	167.13	167.00	136	211	24	15.46	16-jun-03	159.47	163.00	124	188	15	15.62	7-jun-04
Lythrum salicaria	*Purple Loosestrife*	Grote kattenstaart	168.45	167.00	153	189	31	8.93	17-jun-03	177.86	177.00	166	194	28	7.31	25-jun-04
Alopecurus pratensis	*Meadow Foxtail*	Grote vossenstaart								108.94	108.50	90	141	18	13.08	17-apr-04
Glechoma hederacea	*Ground ivy*	Hondsdraf	90.30	89.00	54	111	121	11.26	31-mrt-03	89.11	95.00	14	118	88	21.53	29-mrt-04
Tussilago farfara	*Colt's foot*	Klein hoefblad	68.01	68.00	26	96	155	11.09	9-mrt-03	61.10	61.00	24	106	135	16.85	1-mrt-04
Lychnis flos-cuculi	*Ragged robin*	Koekoeksbloem, Echte, bloei	126.90	127.00	96	157	63	12.16	6-mei-03	130.46	130.00	90	149	52	10.95	9-mei-04
Dactylis glomerata	*Cock's-foot*	Kropaar								130.50	119.00	106	180	10	21.79	9-mei-04
Ranunculus repens	*Creeping buttercup*	Kruipende boterbloem	116.51	118.00	72	141	35	13.87	26-apr-03	119.53	120.00	91	141	40	9.11	28-apr-04
Alliaria petiolata	*Garlic mustard*	Look zonder look	110.47	110.00	94	130	78	6.27	20-apr-03	108.61	109.00	87	125	87	6.05	17-apr-04
Viola odorata	*Sweet violet*	Maarts viooltje	78.65	79.00	54	104	97	9.15	19-mrt-03	70.77	76.00	3	109	95	17.84	10-mrt-04
Leucanthemum vulgaris	*Ox-eye daisy*	Margriet, Gewone, bloei	127.62	127.00	93	146	42	8.73	7-mei-03	131.17	131.00	103	152	29	11.87	10-mei-04
Stachys palustris	*Marsh Woundwort*	Moerasandoorn	172.50	171.00	166	182	4	7.19	21-jun-03	178.27	174.00	167	199	11	10.00	26-jun-04
Filipendula ulmaria	*Meadow-sweet*	Moerasspirea	172.86	171.50	153	203	22	12.80	21-jun-03	171.29	172.00	158	185	21	6.32	19-jun-04
Cardamine pratensis	*Cuckoo-flower, Lady's smock*	Pinksterbloem	95.82	95.00	73	128	176	9.14	5-apr-03	96.97	96.00	45	132	188	8.19	5-apr-04
Ranunculus acris	*Meadow buttercup*	Scherpe boterbloem	116.39	114.00	97	141	46	11.31	26-apr-03	110.21	112.00	86	123	52	8.43	19-apr-04
Galanthus nivalis	*Snow drop*	Sneeuwklokje	28.55	30.00	-38	65	164	19.45	28-jan-03	25.65	26.50	1	47	126	11.40	25-jan-04
Ranunculus ficaria	*Small selandine*	Speenkruid	65.91	68.00	5	105	216	17.91	6-mrt-03	63.85	67.00	18	117	206	16.91	3-mrt-04
Hypericum perforatum	*common St. Johnswort*	St. janskruid	168.18	166.00	134	204	22	13.20	17-jun-03							
Phleum pratense	*Timothy*	Timoteegras								168.75	168.00	154	182	8	8.55	16-jun-04
Daucus carota	*Wild Carrot*	Wilde peen	166.36	172.00	109	187	11	23.26	15-jun-03	175.67	174.00	157	192	9	11.26	23-jun-04
Lamium album	*White deadnettle*	Witte dovenetel	105.90	107.00	76	131	88	10.71	15-apr-03	95.99	100.00	15	120	92	22.16	4-apr-04

Table 8-7. Aggregated vegetation classes

LGN4 class codes	LGN4 Class names	New class codes	New Class names
0	no data	**0**	no data
1	grass	**1**	grass
2, 3, 4	maize, potatoes, beets	**2**	maize, potato, beet
5	cereals	**3**	cereals
6, 9	other agricultural crops, orchards	**4**	other agricultural crops
10	bulb cultivation	**5**	bulb cultivation
11, 43	deciduous forest, forest in swamp areas	**6**	deciduous forest
12	coniferous forest	**7**	coniferous forest
16, 17	fresh water, salt water	**8**	water
18 - 26	continuous urban area, built-up in rural area, deciduous forest in urban area, coniferous forest in urban area, built-up area with dense forest, grass in built-up area, bare soil in built-up area, main roads and railways, buildings in rural area	**9**	built up area
30 – 42; 44 - 46	salt marshes; beaches and dunes; sparcely vegetated dunes; vegetated dunes; heathlands in dune areas; shifting sands; heathlands; heathlands with minor grass influence; heathlands with major grass influence; raised bogs; forest in raised bogs; miscellaneous swamp vegetation; reed swamp; swampy pastures in peat areas; herbaceous vegetation; bare soil in natural areas	**10**	nature area

Table 8-8. VI usefulness Index related to VI quality assessment science datasets (QA SDS).

Bit No.	Parameter Name	Bit Comb.	Description
2-5	VI Usefulness Index	0000	Perfect quality (equal to VI quality = 00: VI produced with good quality)
		0001	High quality
		0010	Good quality
		0011	Acceptable quality
		0100	Fair quality
		0101	Intermediate quality
		0110	Below intermediate quality
		0111	Average quality
		1000	Below average quality
		1001	Questionable quality
		1010	Above marginal quality
		1011	Marginal quality
		1100	Low quality
		1101	No atmospheric correction performed
		1110	Quality too low to be useful
		1111	Not useful for other reasons (equal to VI quality = 11: VI not produced due to bad quality)

Adapted from: http://tbrs.arizona.edu/project/MODIS/UserGuide_doc.php#Fileformat1 (2004).

(a)

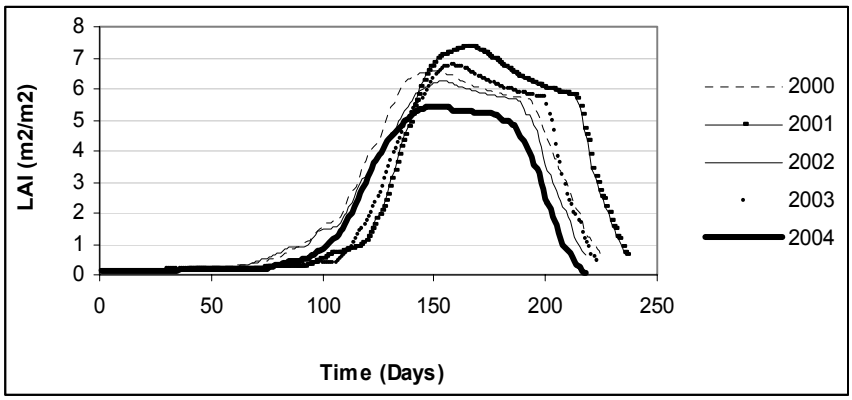

(b)

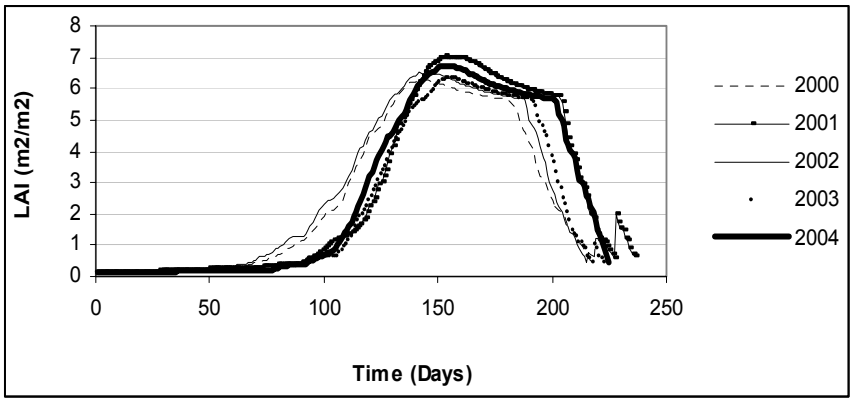

(c)

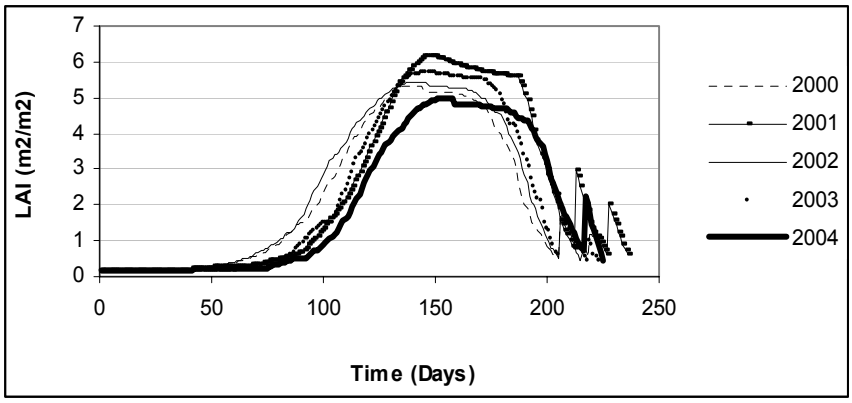

Figure 8-2. Winterwheat WOFOST/CGMS LAI for location North (a), Centre (b) and South (c) from 2000 to 2004

Table 8-9. Remote sensing phenological indicators for forest from 2000 to 2004, according to the different combinations of methods.

Mean (16d unit)	2000		2001		2002		2003		2004	
CV (%)	mean	cv	mean	cv	mean	cv	mean	cv	mean	cv
ndvi_sg_smn_sos	8	8.98	8	11.41	8	9.90	8	9.49	7	12.07
ndvi_hants_smn_sos	8	16.29	8	12.77	8	15.66	8	14.17	7	17.99
ndvi_sg_deriv_sos	8	32.79	7	25.53	8	23.52	7	17.92	8	29.13
ndvi_hants_deriv_sos	8	19.65	8	15.59	8	17.88	8	16.33	7	21.98
evi_sg_smn_sos	8	9.17	8	10.50	8	10.01	8	9.98	8	11.40
evi_hants_smn_sos	7	15.59	8	13.41	7	11.71	7	15.14	7	14.97
evi_sg_deriv_sos	7	16.54	8	17.77	8	16.74	8	13.01	8	16.65
evi_hants_deriv_sos	7	18.46	8	14.37	7	12.97	7	16.91	7	16.39
ndvi_sg_smn_eos	17	32.69	19	28.81	17	36.67	19	27.27	18	32.14
ndvi_hants_smn_eos	19	11.10	20	10.96	18	11.32	19	9.27	20	7.68
ndvi_sg_deriv_eos	19	18.79	20	11.94	19	17.44	20	21.71	19	26.55
ndvi_hants_deriv_eos	19	10.98	20	9.26	18	8.15	19	8.39	20	7.37
evi_sg_smn_eos	18	14.32	18	9.52	17	13.78	18	10.18	18	12.06
evi_hants_smn_eos	19	8.37	18	6.58	17	5.92	18	6.94	18	7.65
evi_sg_deriv_eos	18	15.86	18	11.07	17	12.94	17	12.70	17	16.41
evi_hants_deriv_eos	19	9.52	18	7.06	17	6.97	17	7.61	18	8.98
ndvi_sg_smn_lgs	12	17.15	13	18.37	13	29.01	13	22.19	15	20.73
ndvi_hants_smn_lgs	12	21.80	12	20.20	10	21.51	11	20.19	13	15.51
ndvi_sg_deriv_lgs	13	24.60	14	20.69	12	26.29	13	24.17	16	29.74
ndvi_hants_deriv_lgs	12	26.79	13	23.36	11	29.28	12	25.12	14	19.87
evi_sg_smn_lgs	10	19.84	10	15.71	10	17.03	9	18.32	10	18.23
evi_hants_smn_lgs	11	19.67	9	17.22	9	16.56	10	18.33	10	21.02
evi_sg_deriv_lgs	11	23.71	10	20.41	9	22.75	9	28.74	10	32.42
evi_hants_deriv_lgs	12	23.33	10	23.27	9	20.63	10	21.61	11	24.89

Table 8-10. Remote sensing phenological indicators for grassland from 2000 to 2004, according to the different combinations of methods.

Mean (16d unit)	2000		2001		2002		2003		2004	
CV (%)	mean	cv	mean	cv	mean	cv	mean	cv	mean	cv
ndvi_sg_smn_sos	7	36.88	7	24.13	7	28.60	7	17.05	7	29.81
ndvi_hants_smn_sos	8	39.71	7	35.69	7	36.33	7	17.50	6	36.46
ndvi_sg_deriv_sos	12	38.98	9	46.30	10	37.25	7	37.18	12	39.32
ndvi_hants_deriv_sos	12	38.50	9	43.16	10	39.08	7	38.74	8	48.43
evi_sg_smn_sos	7	25.08	7	19.37	7	20.14	7	12.18	6	21.85
evi_hants_smn_sos	7	29.14	7	26.55	6	21.37	6	14.70	6	23.95
evi_sg_deriv_sos	9	41.77	8	41.41	8	37.35	7	23.12	9	41.39
evi_hants_deriv_sos	7	39.91	7	33.22	6	29.00	6	24.82	6	33.97
ndvi_sg_smn_eos	11	45.44	12	42.85	13	50.60	15	33.99	15	40.30
ndvi_hants_smn_eos	13	40.30	16	33.18	15	33.88	17	23.90	18	26.75
ndvi_sg_deriv_eos	16	33.71	14	35.84	15	33.80	15	30.22	17	29.79
ndvi_hants_deriv_eos	17	27.15	18	24.14	17	22.88	17	23.15	20	16.34
evi_sg_smn_eos	14	33.75	15	31.17	16	30.28	15	21.88	15	33.14
evi_hants_smn_eos	19	19.73	18	18.22	18	16.04	16	19.04	18	17.57
evi_sg_deriv_eos	16	28.33	15	29.69	15	27.81	14	22.63	16	27.61
evi_hants_deriv_eos	19	16.06	18	16.67	18	16.13	16	19.71	18	15.75
ndvi_sg_smn_lgs	10	45.79	11	50.44	13	50.30	12	48.07	18	31.08
ndvi_hants_smn_lgs	9	41.24	10	38.92	11	37.80	11	37.29	13	31.59
ndvi_sg_deriv_lgs	10	47.14	10	48.35	10	45.24	11	45.01	18	31.32
ndvi_hants_deriv_lgs	10	43.74	11	41.23	11	41.12	12	38.76	14	34.08
evi_sg_smn_lgs	10	36.73	10	35.95	11	40.04	8	40.20	13	37.92
evi_hants_smn_lgs	12	28.75	12	28.48	11	27.20	9	32.47	12	27.65
evi_sg_deriv_lgs	11	43.09	11	40.20	10	44.36	9	44.18	16	37.44
evi_hants_deriv_lgs	13	33.60	13	33.44	12	31.34	10	34.81	13	31.90

Table 8-11. Remote sensing phenological indicators for winter wheat from 2000 to 2004, according to the different combinations of methods.

Mean (16d unit)	2000		2001		2002		2003		2004	
CV (%)	mean	cv	mean	cv	mean	cv	mean	cv	mean	cv
ndvi_sg_smn_sos	8	16.43	9	18.09	9	14.30	8	12.27	7	22.88
ndvi_hants_smn_sos	8	25.61	9	21.45	8	18.59	8	13.02	7	20.86
ndvi_sg_deriv_sos	10	40.92	9	30.96	9	28.66	8	31.69	9	46.63
ndvi_hants_deriv_sos	10	47.20	10	33.26	9	34.65	8	28.08	7	34.90
evi_sg_smn_sos	8	19.49	9	18.33	8	15.87	8	12.43	7	19.16
evi_hants_smn_sos	7	23.15	8	19.60	8	18.64	8	13.15	7	17.88
evi_sg_deriv_sos	8	29.77	8	24.23	9	19.08	8	19.39	8	30.40
evi_hants_deriv_sos	7	27.16	8	19.20	7	21.15	7	15.18	7	21.55
ndvi_sg_smn_eos	13	39.89	14	44.47	14	40.85	16	18.91	16	23.08
ndvi_hants_smn_eos	16	20.94	17	18.77	16	17.81	16	14.85	17	19.55
ndvi_sg_deriv_eos	16	25.21	17	20.44	16	26.73	15	21.86	16	23.39
ndvi_hants_deriv_eos	16	19.15	17	14.32	16	13.23	16	14.33	17	19.69
evi_sg_smn_eos	15	18.91	16	17.56	15	18.64	15	13.47	15	17.62
evi_hants_smn_eos	16	14.69	17	10.98	16	12.41	16	11.84	16	14.26
evi_sg_deriv_eos	15	19.15	16	16.45	15	17.91	15	14.01	15	17.25
evi_hants_deriv_eos	16	15.55	17	11.01	16	12.80	16	12.11	16	15.19
ndvi_sg_smn_lgs	9	33.43	10	43.32	9	45.04	7	34.69	9	34.19
ndvi_hants_smn_lgs	10	30.72	9	29.99	9	31.98	9	35.21	10	31.73
ndvi_sg_deriv_lgs	9	43.04	10	37.06	9	50.71	8	43.29	10	48.51
ndvi_hants_deriv_lgs	9	43.11	9	37.83	9	38.26	9	38.63	10	37.39
evi_sg_smn_lgs	7	29.25	8	27.96	7	32.06	6	29.79	8	30.62
evi_hants_smn_lgs	9	25.42	8	22.88	8	24.69	8	24.84	9	25.85
evi_sg_deriv_lgs	8	38.57	8	36.37	7	45.40	7	33.01	8	41.06
evi_hants_deriv_lgs	9	31.58	8	29.62	8	29.52	8	27.62	9	31.53

a)

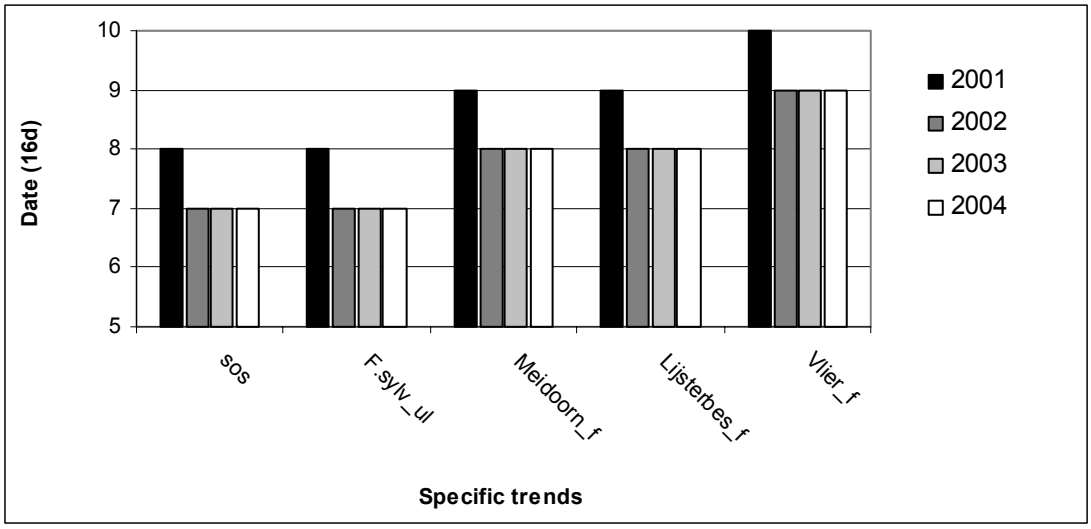

b)

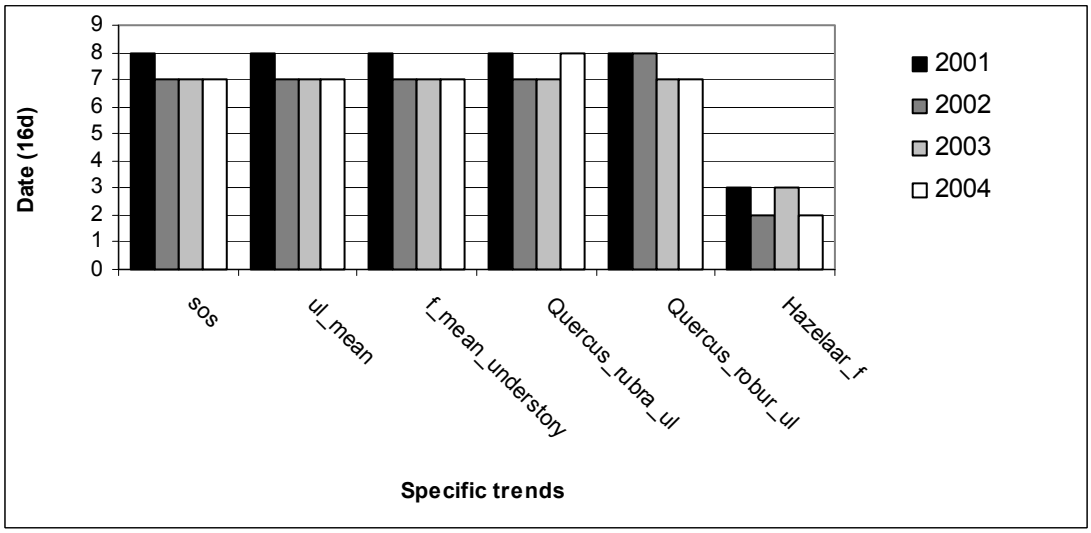

Figure 8-3. Overview of the comparison of the Mean RS SOS dates and the Mean UL and F dates of forest species

a) Leaf unfolding trend of the *Fagus sylvatica.* Flowering trend of the Meidoorn, the Lijsterbes and the Vlier. b) The methods also followed the UL trend of the other species, however, UL dates did not fell in the 16d interval of the found SOS trend. SOS = ***evi_hants_smn*** and **the *evi_hants_deriv***